Synthesis and Structural Characterisation of the Osmium Cluster Dianions $[Os_{17}(CO)_{36}]^{2-}$ and $[Os_{20}(CO)_{40}]^{2-}$†

Lutz H. Gade,[a] Brian F. G. Johnson,*[,b] Jack Lewis,*[,a] Mary McPartlin,*[,c] Harold R. Powell,[c] Paul R. Raithby[a] and Wing-Tak Wong[a]

[a] *University Chemical Laboratory, Lensfield Road, Cambridge CB2 1EW, UK*

[b] *Chemistry Department, University of Edinburgh, Kings Buildings, West Mains Road, Edinburgh EH9 3JJ, UK*

[c] *School of Chemistry, University of North London, Holloway Road, London N7 8DB, UK*

The cluster dianions $[Os_{17}(CO)_{36}]^{2-}$ and $[Os_{20}(CO)_{40}]^{2-}$, the largest osmium carbonyl clusters isolated to date, have been obtained by vacuum pyrolysis of $[Os_3(CO)_{10}(NCMe)_2]$ at temperatures above 260 °C and initial pressures of *ca.* 10^{-3} Torr. A single-crystal X-ray structure analysis of $[AsPh_4]_2[Os_{17}(CO)_{36}]$ has established a trigonal-bipyramidal core of 14 osmium atoms which is capped by three additional Os atoms. Carbon-13 NMR studies indicate a high degree of fluxionality in the cluster. The crystal structure analysis of $[PBu^n_4]_2[Os_{20}(CO)_{40}]$ has revealed a tetrahedral cubic close-packed metal core of twenty osmium atoms which represents the first example of a totally symmetrical array of metal atoms of this nuclearity, a geometrical arrangement previously proposed for both bare and ligated eicosanuclear metal clusters. The structure of the latter bears close resemblance to the chemisorption of CO on metal (111) surfaces at high density. An interpretation of some aspects of its redox chemical behaviour on the basis of the electronic structure of the compound is given.

The chemistry of polynuclear metal carbonyls has expanded enormously during the past two decades and has produced a considerable number of high-nuclearity clusters containing up to a few dozen metal atoms.[1] The growing number of structurally characterised species has fuelled an increased interest in their chemical and physicochemical properties.[2] They provide models for the chemisorption of CO (or, in the case of hydridocarbonyl clusters, CO and H_2, *i.e.* 'synthesis gas') on the surface of colloidal metal particles or even bulk metals, and as a consequence their study has been the basis of a fruitful interaction between inorganic chemistry and surface science as well as small-particle physics.[3] The suitability of cluster complexes as model systems lies in the fact that they are strictly monodispersed and as molecular species can be purified by well established experimental techniques. Moreover, since the exact nuclearity and geometry is known for most of the compounds studied, a direct correlation between structure and physical properties should at least in principle be possible.

While our knowledge of the structural features of clusters with large metal cores has been greatly enhanced by the wealth of information gained from single-crystal X-ray diffraction and spectroscopic studies in solution, the development of systematic methodologies for the synthesis of these compounds lags far behind. The complexity of the bonding and co-ordination modes adopted by transition-metal compounds and the relative similarity of the M–M, M–CO and M–H bond energies may lie at the root of this problem.[4] The current syntheses of monometallic high-nuclearity clusters are based on the recombination of reactive fragments generated from appropriate precursors either by thermal or redox processes.[5] From the point of view of developing a synthetic strategy both methods may appear unsatisfactory. However, thermolytic syntheses of one kind or another have been very successful for clusters of virtually all metals of the iron, cobalt and nickel triads leading to a large and varied spectrum of metal cores some of which display highly symmetrical geometries.[6] The method has been used extensively in the synthesis of ruthenium and osmium clusters. The most important precursor materials in this area are the trinuclear metal carbonyls or their substituted derivatives for which reaction conditions have been found that lead to a range of clusters containing between four and twenty metal atoms.

In this paper we report what at present represents the top end of the nuclearity scale in osmium cluster chemistry, the preparation and characterisation of two novel high-nuclearity cluster dianions as products in the vacuum pyrolysis of $[Os_3(CO)_{10}(NCMe)_2]$.[7]

Results and Discussion

Pyrolysis of $[Os_3(CO)_{10}(NCMe)_2]$ *at High Temperatures.*—The vacuum pyrolysis of $[Os_3(CO)_{10}(NCMe)_2]$, an activated derivative of the binary carbonyl, at temperatures above 260 °C has been used previously for the synthesis of $[Os_{10}C(CO)_{24}]^{2-}$ **1**.[8] Although high yields of **1** {as its $[N(PPh_3)_2]^+$ salt} may be obtained occasionally, this method has generally proved to be less efficient (yields of **1** ranging between 20 and 40%) than the original synthesis employing $[Os_3(CO)_{11}(py)]$ (py = pyridine) (65–70% of **1**).[9]

While $[Os_3(CO)_{10}(NCMe)_2]$ is thus not the ideal precursor of **1**, a systematic investigation of the high-nuclearity fractions generated at temperatures between 260 and 300 °C has led to the isolation and characterisation of new high-nuclearity clusters, namely the dianions $[Os_{17}(CO)_{36}]^{2-}$ and $[Os_{20}(CO)_{40}]^{2-}$.

Synthesis, Structure and Properties of $[Os_{17}(CO)_{36}]^{2-}$.—The isolation of pure salts of $[Os_{10}C(CO)_{24}]^{2-}$ **1** from the pyrolysis of $[Os_3(CO)_{10}(NCMe)_2]$ has previously been impeded by a minor cluster component which has similar chromatographic properties on silica. In large-scale preparations in particular, this purification problem has been responsible for substantial reductions in the yield of isolated **1**. The dark brown anionic

† *Supplementary data available:* see Instructions for Authors, *J. Chem. Soc., Dalton Trans.*, 1994, Issue 1, pp. xxiii–xxviii.

Non-SI unit employed: Torr ≈ 133 Pa.

'impurity' could, however, be fully separated from **1** by repeated TLC separation on silica (eluent, acetone–hexane (60:40); R_f = 0.60–0.65) and thus obtained in overall yields of up to 10%.

The negative-ion FAB mass spectrum of the $[AsPh_4]^+$ salt of this new cluster fraction displayed the characteristic pattern found for cluster dianions, with three prominent isotope peak distributions centred around the most abundant isotopomers at m/z = 2121, 4242 and 4626. These data are consistent with the formulation of the cluster as $[Os_{17}(CO)_{36}]^{2-}$ **2**, the three peaks representing the dianion (simulation: m/z 2122), the monoanion (simulation: m/z 4245) and the ion pair $[\{Os_{17}(CO)_{36}\}(AsPh_4)]^-$ (simulation: m/z 4628). Similar mass spectra were recorded of the $[N(PPh_3)_2]^+$ and $[PMePh_3]^+$ salts. The position of the ν(CO) absorption bands in the IR spectrum of the cluster (see Experimental section) is in accord with the formulation as a dianion however the complicated band pattern precluded any structural assignment.

Crystals suitable for X-ray crystallography were obtained from the $[AsPh_4]^+$ salt. The molecular structure of the cluster dianion is shown in Fig. 1(*a*), the bare metal framework is depicted in Fig. 1(*b*) and the principal bond distances and interbond angles are listed in Table 1. The structure of the cluster contains a close-packed metal core of 16 Os atoms and a slightly displaced seventeenth metal atom which breaks the otherwise three-fold symmetry of the system. The stacking sequences of both cubic and hexagonal close-packed lattices are combined to give an overall ABCBA stacking, in contrast to the hexagonal close packing observed in the bulk metal. The structure may be described as containing two face-sharing tetrahedra (*i.e.* a trigonal bipyramid) of 14 Os atoms with three metal atoms capping the central Os_3 triangles of the faces of one tetrahedron. One cap is distorted to form an extra bond to one of the equatorial vertices of the trigonal bipyramid. This results in two extremely long Os–Os 'bonds' [Os(17)–Os(2) 3.152(5) and Os(17)–Os(10) 3.140(4) Å]. The small component of disorder in the cluster (see Experimental section) means that some caution is required in considering the Os–Os distances. However, a prominent feature of the metal framework is the high metal–metal connectivity of eight and nine of the Os atoms in the octahedron comprising Os(1)–Os(6), and it appears that these unusual metal–metal environments are associated with some very short Os–Os distances, $d_{av}(Os–Os)_{oct}$ = 2.663 Å which is very similar to the Os–Os distance observed in the bulk metal, d(Os–Os) = 2.6754 Å.[10] In comparison to that, the average bond distance between the Os atoms of the fused second octahedron [Os(4)–Os(9)] is 2.743 Å.

The metal–metal distances within the osmium framework along with the absence of any significant electron density at the centres of the polyhedral subunits confirms the formulation of the cluster without interstitial ligands (as was established independently by ^1H and ^{13}C NMR spectroscopy). Interstitial carbido atoms, for example, tend to induce an expansion of the cavity in which they reside. This is exemplified by the structures of the two tetracapped-octahedral cluster dianions $[Os_{10}C(CO)_{24}]^{2-}$ **1** and $[Os_{10}H_4(CO)_{24}]^{2-}$. The average Os–Os distance in the central octahedron of the former is 2.883 Å,[9] while that of the tetrahydrido cluster, for which a neutron diffraction study has unambiguously established the absence of interstitial atoms, was found to be 2.840 Å.[11] As has been pointed out above, the two inequivalent octahedral sites in **2** are even more contracted.

The wide variation of metal–metal distances observed in this structure (2.567–3.152 Å) makes questionable an analysis of the cluster geometry within the set of rules of the polyhedral skeletal electron pair theory (PSEPT),[12] which treats all these Os–Os contacts as 'metal–metal bonds'. The structure of cluster **2** must therefore be regarded as a borderline case for the meaningful application of the PSEPT for condensed polyhedra. Nevertheless, if one assumes an electron count of 122 for the two face-sharing octahedra at the centre of the metal core {as found, for instance, in $[Rh_9(CO)_{19}]^{3-}$ (ref. 13)} and takes the additional metal–metal bond of the distorted cap into account, the overall c.v.e. (cluster valence electron) count of 210 is in agreement with the PSEPT.

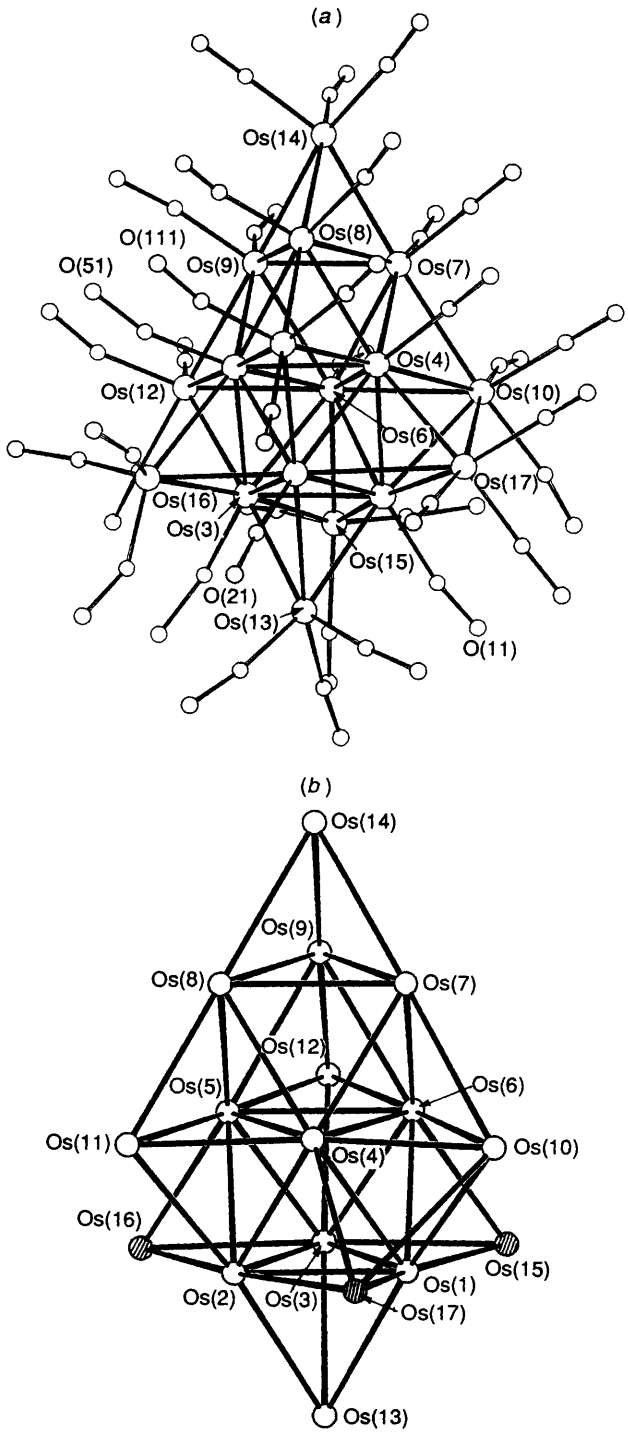

Fig. 1 (*a*) Molecular structure of the dianion $[Os_{17}(CO)_{36}]^{2-}$ **2**. (*b*) The tricapped trigonal-bipyramidal framework in **2**. One of the caps, Os(17), is asymmetric and is bonded to four metal atoms [Os(1), Os(2), Os(4) and Os(10)]

In view of the broken symmetry of the cluster in the solid state it was of interest whether this situation was retained in solution. The ^{13}CO signal pattern in the ^{13}C NMR spectrum of cluster **2** recorded in CD_2Cl_2 at 300 K (Fig. 2) exhibits a higher symmetry of the cluster than anticipated from its solid-state structure. The partial assignment of the signals is based on their relative intensities and the observation that for many high-

Table 1 Principal bond lengths (Å) and angles (°) for cluster **2**

Os(1)–Os(2)	2.567(3)	Os(1)–Os(3)	2.584(4)	Os(4)–Os(17)	2.676(4)	Os(4)–Os(18)	2.629(14)
Os(1)–Os(4)	2.740(4)	Os(1)–Os(6)	2.595(3)	Os(4)–Os(6)	2.724(3)	Os(5)–Os(6)	2.763(3)
Os(1)–Os(10)	2.772(4)	Os(1)–Os(13)	2.759(3)	Os(5)–Os(8)	2.767(4)	Os(5)–Os(9)	2.757(3)
Os(1)–Os(15)	2.765(3)	Os(1)–Os(17)	2.674(5)	Os(5)–Os(11)	2.792(4)	Os(5)–Os(12)	2.795(3)
Os(1)–Os(18)	3.186(17)	Os(3)–Os(5)	2.668(4)	Os(5)–Os(16)	2.768(3)	Os(6)–Os(15)	2.775(4)
Os(2)–Os(3)	2.600(3)	Os(2)–Os(4)	2.662(3)	Os(6)–Os(7)	2.734(4)	Os(6)–Os(9)	2.778(3)
Os(2)–Os(5)	2.636(3)	Os(2)–Os(11)	2.789(4)	Os(6)–Os(10)	2.868(4)	Os(6)–Os(12)	2.809(4)
Os(2)–Os(13)	2.773(4)	Os(2)–Os(16)	2.800(4)	Os(7)–Os(8)	2.767(4)	Os(7)–Os(9)	2.728(4)
Os(2)–Os(17)	3.152(5)	Os(2)–Os(18)	2.662(20)	Os(7)–Os(10)	2.848(4)	Os(7)–Os(14)	2.795(4)
Os(3)–Os(6)	2.711(3)	Os(3)–Os(12)	2.763(3)	Os(8)–Os(9)	2.723(4)	Os(8)–Os(11)	2.800(3)
Os(3)–Os(13)	2.794(3)	Os(3)–Os(15)	2.741(4)	Os(8)–Os(14)	2.789(3)	Os(9)–Os(12)	2.761(4)
Os(3)–Os(16)	2.719(4)	Os(4)–Os(5)	2.711(4)	Os(9)–Os(14)	2.788(4)	Os(10)–Os(17)	3.140(4)
Os(4)–Os(7)	2.736(3)	Os(4)–Os(8)	2.732(4)	Os(11) ··· Os(18)	3.389(19)	Os(17) ··· Os(18)	1.139(18)
Os(4)–Os(10)	2.731(4)	Os(4)–Os(11)	2.753(4)	Os–C (mean)	1.85(8)	C–O (mean)	1.17(9)
Os(3)–Os(1)–Os(2)	60.6(1)	Os(4)–Os(1)–Os(2)	60.1(1)	Os(6)–Os(5)–Os(2)	87.3(1)	Os(6)–Os(5)–Os(3)	59.9(1)
Os(4)–Os(1)–Os(3)	92.0(1)	Os(6)–Os(1)–Os(2)	92.5(1)	Os(6)–Os(5)–Os(4)	59.7(1)	Os(8)–Os(5)–Os(2)	110.5(1)
Os(6)–Os(1)–Os(3)	63.1(1)	Os(6)–Os(1)–Os(4)	61.3(1)	Os(8)–Os(5)–Os(3)	146.8(1)	Os(8)–Os(5)–Os(4)	59.8(1)
Os(10)–Os(1)–Os(2)	119.1(1)	Os(10)–Os(1)–Os(3)	127.5(1)	Os(8)–Os(5)–Os(6)	89.9(1)	Os(9)–Os(5)–Os(2)	144.4(1)
Os(10)–Os(1)–Os(4)	59.4(1)	Os(10)–Os(1)–Os(6)	64.5(1)	Os(9)–Os(5)–Os(3)	109.5(1)	Os(9)–Os(5)–Os(4)	89.2(1)
Os(13)–Os(1)–Os(2)	62.6(1)	Os(13)–Os(1)–Os(3)	62.9(1)	Os(9)–Os(5)–Os(6)	60.4(1)	Os(9)–Os(5)–Os(8)	59.1(1)
Os(13)–Os(1)–Os(4)	122.6(1)	Os(13)–Os(1)–Os(6)	126.0(1)	Os(11)–Os(5)–Os(2)	61.7(1)	Os(11)–Os(5)–Os(3)	120.4(1)
Os(13)–Os(1)–Os(10)	169.4(1)	Os(15)–Os(1)–Os(2)	122.1(1)	Os(11)–Os(5)–Os(4)	60.0(1)	Os(11)–Os(5)–Os(6)	119.7(1)
Os(15)–Os(1)–Os(3)	61.5(1)	Os(15)–Os(1)–Os(4)	123.6(1)	Os(11)–Os(5)–Os(8)	60.5(1)	Os(11)–Os(5)–Os(9)	119.5(1)
Os(15)–Os(1)–Os(6)	62.3(1)	Os(15)–Os(1)–Os(10)	96.8(1)	Os(12)–Os(5)–Os(2)	119.4(1)	Os(12)–Os(5)–Os(3)	60.7(1)
Os(15)–Os(1)–Os(13)	90.2(1)	Os(17)–Os(1)–Os(2)	73.9(1)	Os(12)–Os(5)–Os(4)	120.3(1)	Os(12)–Os(5)–Os(6)	60.7(1)
Os(17)–Os(1)–Os(3)	134.3(1)	Os(17)–Os(1)–Os(4)	59.2(1)	Os(12)–Os(5)–Os(8)	118.7(1)	Os(12)–Os(5)–Os(9)	59.6(1)
Os(17)–Os(1)–Os(6)	117.5(1)	Os(17)–Os(1)–Os(10)	70.4(1)	Os(12)–Os(5)–Os(11)	178.9(1)	Os(16)–Os(5)–Os(2)	62.3(1)
Os(17)–Os(1)–Os(13)	101.2(1)	Os(17)–Os(1)–Os(15)	163.6(1)	Os(16)–Os(5)–Os(3)	60.0(1)	Os(16)–Os(5)–Os(4)	122.0(1)
Os(4)–Os(2)–Os(1)	63.2(1)	Os(4)–Os(2)–Os(3)	93.4(1)	Os(16)–Os(5)–Os(6)	119.8(1)	Os(16)–Os(5)–Os(8)	147.5(1)
Os(5)–Os(2)–Os(1)	91.8(1)	Os(5)–Os(2)–Os(3)	61.3(1)	Os(16)–Os(5)–Os(9)	145.4(1)	Os(16)–Os(5)–Os(11)	91.2(1)
Os(5)–Os(2)–Os(4)	61.6(1)	Os(11)–Os(2)–Os(1)	123.8(1)	Os(16)–Os(5)–Os(12)	89.4(1)	Os(15)–Os(6)–Os(10)	94.3(1)
Os(11)–Os(2)–Os(3)	123.1(1)	Os(11)–Os(2)–Os(4)	60.6(1)	Os(3)–Os(6)–Os(1)	58.2(1)	Os(4)–Os(6)–Os(1)	62.0(1)
Os(11)–Os(2)–Os(5)	61.9(1)	Os(13)–Os(2)–Os(1)	62.1(1)	Os(4)–Os(6)–Os(3)	89.6(1)	Os(5)–Os(6)–Os(1)	88.4(1)
Os(13)–Os(2)–Os(3)	62.6(1)	Os(13)–Os(2)–Os(4)	125.1(1)	Os(5)–Os(6)–Os(3)	58.3(1)	Os(5)–Os(6)–Os(4)	59.2(1)
Os(13)–Os(2)–Os(5)	123.7(1)	Os(13)–Os(2)–Os(11)	172.9(1)	Os(7)–Os(6)–Os(1)	112.5(1)	Os(7)–Os(6)–Os(3)	145.6(1)
Os(16)–Os(2)–Os(1)	120.3(1)	Os(16)–Os(2)–Os(3)	60.3(1)	Os(7)–Os(6)–Os(4)	60.2(1)	Os(7)–Os(6)–Os(5)	90.1(1)
Os(16)–Os(2)–Os(4)	122.7(1)	Os(16)–Os(2)–Os(5)	61.1(1)	Os(9)–Os(6)–Os(1)	145.4(1)	Os(9)–Os(6)–Os(3)	107.7(1)
Os(16)–Os(2)–Os(11)	90.7(1)	Os(16)–Os(2)–Os(13)	89.0(1)	Os(9)–Os(6)–Os(4)	88.5(1)	Os(9)–Os(6)–Os(5)	59.7(1)
Os(17)–Os(2)–Os(1)	54.6(1)	Os(17)–Os(2)–Os(3)	114.5(1)	Os(9)–Os(6)–Os(7)	59.3(1)	Os(10)–Os(6)–Os(1)	60.7(1)
Os(17)–Os(2)–Os(4)	54.0(1)	Os(17)–Os(2)–Os(5)	115.2(1)	Os(10)–Os(6)–Os(3)	118.9(1)	Os(10)–Os(6)–Os(4)	58.4(1)
Os(17)–Os(2)–Os(11)	90.9(1)	Os(17)–Os(2)–Os(13)	90.1(1)	Os(10)–Os(6)–Os(5)	117.6(1)	Os(10)–Os(6)–Os(7)	61.1(1)
Os(17)–Os(2)–Os(16)	174.4(1)	Os(2)–Os(3)–Os(1)	59.4(1)	Os(10)–Os(6)–Os(9)	120.3(1)	Os(12)–Os(6)–Os(1)	118.3(1)
Os(5)–Os(3)–Os(2)	60.1(1)	Os(6)–Os(3)–Os(1)	58.6(1)	Os(12)–Os(6)–Os(3)	60.0(1)	Os(12)–Os(6)–Os(4)	119.4(1)
Os(6)–Os(3)–Os(2)	89.2(1)	Os(6)–Os(3)–Os(5)	61.8(1)	Os(12)–Os(6)–Os(5)	60.2(1)	Os(12)–Os(6)–Os(7)	118.5(1)
Os(12)–Os(3)–Os(1)	120.4(1)	Os(12)–Os(3)–Os(2)	122.0(1)	Os(12)–Os(6)–Os(9)	59.2(1)	Os(12)–Os(6)–Os(10)	177.8(1)
Os(12)–Os(3)–Os(5)	61.9(1)	Os(12)–Os(3)–Os(6)	61.7(1)	Os(15)–Os(6)–Os(1)	61.9(1)	Os(15)–Os(6)–Os(3)	59.9(1)
Os(13)–Os(3)–Os(1)	61.6(1)	Os(13)–Os(3)–Os(2)	61.8(1)	Os(15)–Os(6)–Os(4)	123.8(1)	Os(15)–Os(6)–Os(5)	118.2(1)
Os(13)–Os(3)–Os(5)	121.7(1)	Os(13)–Os(3)–Os(6)	120.2(1)	Os(15)–Os(6)–Os(7)	149.8(1)	Os(15)–Os(6)–Os(9)	142.8(1)
Os(13)–Os(3)–Os(12)	176.2(1)	Os(15)–Os(3)–Os(1)	62.5(1)	Os(15)–Os(6)–Os(12)	86.7(1)	Os(6)–Os(7)–Os(4)	59.7(1)
Os(15)–Os(3)–Os(2)	121.8(1)	Os(15)–Os(3)–Os(5)	122.9(1)	Os(8)–Os(7)–Os(4)	59.5(1)	Os(8)–Os(7)–Os(6)	90.6(1)
Os(15)–Os(3)–Os(6)	61.2(1)	Os(15)–Os(3)–Os(12)	88.3(1)	Os(9)–Os(7)–Os(4)	89.2(1)	Os(9)–Os(7)–Os(6)	61.1(1)
Os(15)–Os(3)–Os(13)	90.0(1)	Os(16)–Os(3)–Os(1)	122.8(1)	Os(9)–Os(7)–Os(8)	59.4(1)	Os(10)–Os(7)–Os(4)	58.5(1)
Os(16)–Os(3)–Os(2)	63.5(1)	Os(16)–Os(3)–Os(5)	61.8(1)	Os(10)–Os(7)–Os(6)	61.8(1)	Os(10)–Os(7)–Os(8)	117.9(1)
Os(16)–Os(3)–Os(6)	123.6(1)	Os(16)–Os(3)–Os(12)	91.1(1)	Os(10)–Os(7)–Os(9)	122.8(1)	Os(14)–Os(7)–Os(4)	119.7(1)
Os(16)–Os(3)–Os(13)	90.2(1)	Os(16)–Os(3)–Os(15)	173.8(1)	Os(14)–Os(7)–Os(6)	121.8(1)	Os(14)–Os(7)–Os(8)	60.2(1)
Os(5)–Os(3)–Os(1)	90.7(1)	Os(2)–Os(4)–Os(1)	56.7(1)	Os(14)–Os(7)–Os(9)	60.6(1)	Os(14)–Os(7)–Os(10)	175.2(1)
Os(5)–Os(4)–Os(2)	58.8(1)	Os(6)–Os(4)–Os(1)	56.7(1)	Os(7)–Os(8)–Os(4)	59.7(1)	Os(7)–Os(8)–Os(5)	89.4(1)
Os(6)–Os(4)–Os(2)	87.6(1)	Os(6)–Os(4)–Os(5)	61.1(1)	Os(9)–Os(8)–Os(4)	89.4(1)	Os(9)–Os(8)–Os(5)	60.3(1)
Os(7)–Os(4)–Os(1)	108.0(1)	Os(7)–Os(4)–Os(2)	144.9(1)	Os(9)–Os(8)–Os(7)	59.6(1)	Os(11)–Os(8)–Os(4)	59.7(1)
Os(7)–Os(4)–Os(5)	91.2(1)	Os(7)–Os(4)–Os(6)	60.1(1)	Os(11)–Os(8)–Os(5)	60.2(1)	Os(11)–Os(8)–Os(7)	119.4(1)
Os(8)–Os(4)–Os(1)	143.9(1)	Os(8)–Os(4)–Os(2)	110.8(1)	Os(11)–Os(8)–Os(9)	120.5(1)	Os(14)–Os(8)–Os(4)	120.1(1)
Os(8)–Os(4)–Os(5)	61.1(1)	Os(8)–Os(4)–Os(6)	91.5(1)	Os(14)–Os(8)–Os(5)	121.1(1)	Os(14)–Os(8)–Os(7)	60.4(1)
Os(8)–Os(4)–Os(7)	60.8(1)	Os(10)–Os(4)–Os(1)	60.9(1)	Os(14)–Os(8)–Os(9)	60.8(1)	Os(14)–Os(8)–Os(11)	178.5(1)
Os(10)–Os(4)–Os(2)	117.2(1)	Os(10)–Os(4)–Os(5)	124.5(1)	Os(5)–Os(8)–Os(4)	59.1(1)	Os(6)–Os(9)–Os(5)	59.9(1)
Os(10)–Os(4)–Os(6)	63.4(1)	Os(10)–Os(4)–Os(7)	62.8(1)	Os(7)–Os(9)–Os(5)	90.4(1)	Os(7)–Os(9)–Os(6)	59.5(1)
Os(10)–Os(4)–Os(8)	123.4(1)	Os(11)–Os(4)–Os(1)	118.7(1)	Os(8)–Os(9)–Os(5)	60.7(1)	Os(8)–Os(9)–Os(6)	90.6(1)
Os(11)–Os(4)–Os(2)	62.0(1)	Os(11)–Os(4)–Os(5)	61.4(1)	Os(8)–Os(9)–Os(7)	61.0(1)	Os(12)–Os(9)–Os(5)	60.9(1)
Os(11)–Os(4)–Os(6)	122.6(1)	Os(11)–Os(4)–Os(7)	122.2(1)	Os(12)–Os(9)–Os(6)	61.0(1)	Os(12)–Os(9)–Os(7)	120.5(1)
Os(11)–Os(4)–Os(8)	61.4(1)	Os(11)–Os(4)–Os(10)	173.2(1)	Os(12)–Os(9)–Os(8)	121.5(1)	Os(14)–Os(9)–Os(5)	121.4(1)
Os(17)–Os(4)–Os(1)	59.2(1)	Os(17)–Os(4)–Os(2)	72.4(1)	Os(14)–Os(9)–Os(6)	120.4(1)	Os(14)–Os(9)–Os(7)	60.9(1)
Os(17)–Os(4)–Os(5)	130.6(1)	Os(17)–Os(4)–Os(6)	113.1(1)	Os(14)–Os(9)–Os(8)	60.8(1)	Os(14)–Os(9)–Os(12)	177.6(1)
Os(17)–Os(4)–Os(7)	130.7(1)	Os(17)–Os(4)–Os(8)	155.3(1)	Os(6)–Os(10)–Os(1)	54.8(1)	Os(6)–Os(10)–Os(4)	58.2(1)
Os(17)–Os(4)–Os(10)	71.0(1)	Os(17)–Os(4)–Os(11)	102.8(1)	Os(7)–Os(10)–Os(1)	104.1(1)	Os(7)–Os(10)–Os(4)	58.7(1)
Os(5)–Os(4)–Os(1)	86.5(1)	Os(3)–Os(5)–Os(2)	58.7(1)	Os(7)–Os(10)–Os(6)	57.2(1)	Os(17)–Os(10)–Os(1)	53.3(1)
Os(4)–Os(5)–Os(2)	59.7(1)	Os(4)–Os(5)–Os(3)	90.8(1)	Os(17)–Os(10)–Os(4)	53.7(1)	Os(17)–Os(10)–Os(6)	97.1(1)

Table 1 (*continued*)

Os(17)–Os(10)–Os(7)	110.3(1)	Os(4)–Os(10)–Os(1)	59.7(1)	Os(3)–Os(13)–Os(2)	55.7(1)	Os(8)–Os(14)–Os(7)	59.4(1)
Os(5)–Os(11)–Os(2)	56.4(1)	Os(5)–Os(11)–Os(4)	58.5(1)	Os(9)–Os(14)–Os(7)	58.5(1)	Os(9)–Os(14)–Os(8)	58.4(1)
Os(8)–Os(11)–Os(2)	105.2(1)	Os(8)–Os(11)–Os(4)	58.9(1)	Os(3)–Os(15)–Os(1)	56.0(1)	Os(6)–Os(15)–Os(1)	55.9(1)
Os(4)–Os(11)–Os(2)	57.4(1)	Os(8)–Os(11)–Os(5)	59.3(1)	Os(6)–Os(15)–Os(3)	58.9(1)	Os(3)–Os(16)–Os(2)	56.2(1)
Os(5)–Os(12)–Os(3)	57.4(1)	Os(9)–Os(12)–Os(6)	59.8(1)	Os(5)–Os(16)–Os(2)	56.5(1)	Os(5)–Os(16)–Os(3)	58.2(1)
Os(6)–Os(12)–Os(3)	58.2(1)	Os(6)–Os(12)–Os(5)	59.1(1)	Os(2)–Os(17)–Os(1)	51.5(1)	Os(4)–Os(17)–Os(1)	61.6(1)
Os(9)–Os(12)–Os(3)	106.7(1)	Os(9)–Os(12)–Os(5)	59.5(1)	Os(4)–Os(17)–Os(2)	53.6(1)	Os(10)–Os(17)–Os(1)	56.3(1)
Os(2)–Os(13)–Os(1)	55.3(1)	Os(3)–Os(13)–Os(1)	55.5(1)	Os(10)–Os(17)–Os(2)	94.0(1)	Os(10)–Os(17)–Os(4)	55.3(1)

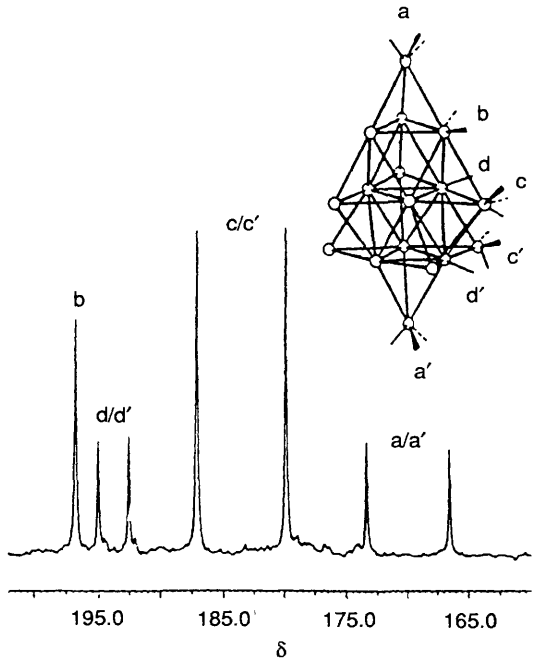

Fig. 2 The ^{13}C NMR spectrum of $[AsPh_4]_2[Os_{17}(CO)_{36}]$ recorded at 300 K in CD_2Cl_2

nuclearity clusters of Os and Ru the resonances of the vertex $M(CO)_3$ carbonyls (M = Ru or Os) appear at higher field than those attached to metal atoms with higher metal–metal connectivity.[14] The simple seven-resonance pattern (see Experimental section) is consistent with an effective C_{3v} symmetry of the species in solution. This indicates that dynamic processes involving both the metal core (dynamic averaging of the distortion of one of the caps) and the ligand shell $[Os(CO)_3$ turnstile rotation, as observed in many other high-nuclearity clusters[14]] must be operative. A low-temperature series of ^{13}C NMR spectra revealed a complicated exchange pattern. Unfortunately, it proved impossible to obtain the low-temperature-limit spectrum even at 180 K. This implies that the observed fluctionality is due to processes with a very low activation barrier.

The assignment of resonance b is unambiguous since there is only one carbonyl environment with six equivalent carbonyl ligands. Based on the chemical shift argument mentioned above, the signals a and a' are interpreted as the resonances of the $Os(CO)_3$ groups at the apical vertices of the trigonal bipyramid while the low-field d/d' signals represent the Os(CO) positions in the cluster. The two intense resonances at δ 187.2 and 179.9 (c/c') must consequently be due to the CO groups on the equatorial vertices of the trigonal bipyramid and the capping $Os(CO)_3$ fragments.

Synthesis, Structure and Reactivity of $[Os_{20}(CO)_{40}]^{2-}$.—Apart from $[Os_{10}C(CO)_{24}]^{2-}$ **1** and $[Os_{17}(CO)_{36}]^{2-}$ **2**, a third major high-nuclearity cluster fraction could be isolated in up to 20% yield from the vacuum pyrolysis of $[Os_3(CO)_{10}(NCMe)_2]$

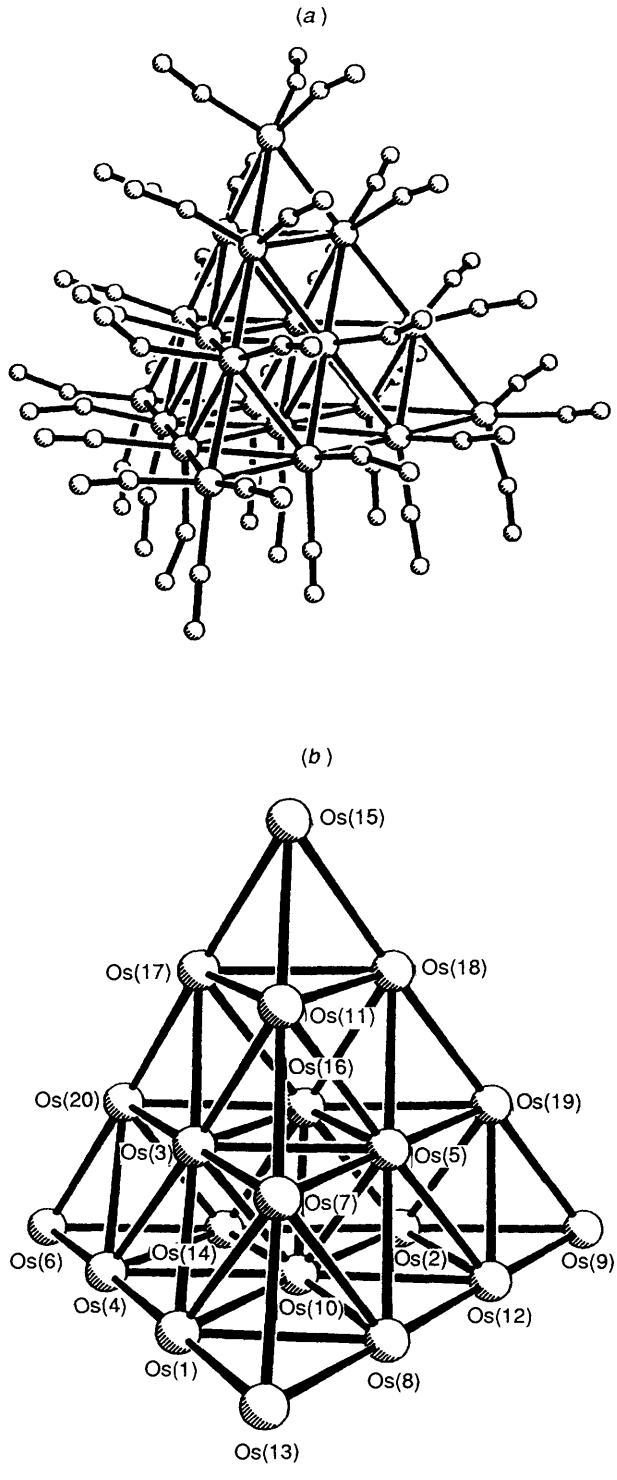

Fig. 3 (*a*) Molecular structure of the dianion $[Os_{20}(CO)_{40}]^{2-}$. (*b*) Structure of the Os_{20} metal core

Table 2 Selected bond lengths (Å) and angles (°) for cluster **3**

Os(1)–Os(3)	2.755(6)	Os(1)–Os(4)	2.754(7)	Os(5)–Os(18)	2.776(6)	Os(5)–Os(19)	2.750(7)
Os(1)–Os(7)	2.742(6)	Os(1)–Os(8)	2.793(7)	Os(6)–Os(14)	2.792(7)	Os(6)–Os(20)	2.807(6)
Os(1)–Os(10)	2.756(7)	Os(1)–Os(13)	2.795(7)	Os(7)–Os(8)	2.753(8)	Os(7)–Os(11)	2.756(6)
Os(2)–Os(9)	2.803(7)	Os(2)–Os(10)	2.793(8)	Os(7)–Os(13)	2.780(6)	Os(8)–Os(10)	2.735(7)
Os(2)–Os(12)	2.761(7)	Os(2)–Os(14)	2.750(7)	Os(8)–Os(12)	2.744(8)	Os(8)–Os(13)	2.809(7)
Os(2)–Os(16)	2.751(8)	Os(2)–Os(19)	2.787(6)	Os(9)–Os(12)	2.802(7)	Os(9)–Os(19)	2.802(7)
Os(3)–Os(4)	2.733(6)	Os(3)–Os(5)	2.685(7)	Os(10)–Os(12)	2.775(7)	Os(10)–Os(14)	2.753(7)
Os(3)–Os(7)	2.788(7)	Os(3)–Os(10)	2.664(8)	Os(10)–Os(16)	2.688(6)	Os(11)–Os(15)	2.790(6)
Os(3)–Os(11)	2.750(6)	Os(3)–Os(16)	2.672(8)	Os(11)–Os(17)	2.794(7)	Os(11)–Os(18)	2.770(8)
Os(3)–Os(17)	2.760(6)	Os(3)–Os(20)	2.788(7)	Os(12)–Os(19)	2.800(6)	Os(14)–Os(16)	2.776(6)
Os(4)–Os(6)	2.778(7)	Os(4)–Os(10)	2.782(7)	Os(14)–Os(20)	2.775(8)	Os(15)–Os(17)	2.811(6)
Os(4)–Os(14)	2.791(8)	Os(4)–Os(20)	2.778(6)	Os(15)–Os(18)	2.774(8)	Os(16)–Os(17)	2.787(8)
Os(5)–Os(7)	2.737(8)	Os(5)–Os(8)	2.785(6)	Os(16)–Os(18)	2.771(6)	Os(16)–Os(19)	2.765(7)
Os(5)–Os(10)	2.669(6)	Os(5)–Os(11)	2.767(8)	Os(16)–Os(20)	2.737(7)	Os(17)–Os(18)	2.771(7)
Os(5)–Os(12)	2.763(8)	Os(5)–Os(16)	2.680(7)	Os(17)–Os(20)	2.750(7)	Os(18)–Os(19)	2.752(8)
Os(3)–Os(1)–Os(4)	59.5(2)	Os(3)–Os(1)–Os(7)	61.0(2)	Os(1)–Os(7)–Os(3)	59.8(2)	Os(1)–Os(7)–Os(5)	90.2(2)
Os(4)–Os(1)–Os(7)	120.4(2)	Os(3)–Os(1)–Os(8)	89.5(2)	Os(3)–Os(7)–Os(5)	58.1(2)	Os(1)–Os(7)–Os(8)	61.1(2)
Os(4)–Os(1)–Os(8)	119.7(2)	Os(7)–Os(1)–Os(8)	59.6(2)	Os(3)–Os(7)–Os(8)	89.7(2)	Os(5)–Os(7)–Os(8)	61.0(2)
Os(3)–Os(1)–Os(10)	57.8(2)	Os(4)–Os(1)–Os(10)	60.6(2)	Os(1)–Os(7)–Os(11)	119.1(2)	Os(3)–Os(7)–Os(11)	59.5(2)
Os(7)–Os(1)–Os(10)	88.2(2)	Os(8)–Os(1)–Os(10)	59.1(2)	Os(5)–Os(7)–Os(11)	60.5(2)	Os(8)–Os(7)–Os(11)	121.4(2)
Os(3)–Os(1)–Os(13)	121.2(2)	Os(4)–Os(1)–Os(13)	179.2(2)	Os(1)–Os(7)–Os(13)	60.8(2)	Os(3)–Os(7)–Os(13)	120.5(2)
Os(7)–Os(1)–Os(13)	60.3(2)	Os(8)–Os(1)–Os(13)	60.3(2)	Os(5)–Os(7)–Os(13)	121.9(2)	Os(8)–Os(7)–Os(13)	61.0(2)
Os(10)–Os(1)–Os(13)	119.4(2)	Os(9)–Os(2)–Os(10)	120.4(2)	Os(11)–Os(7)–Os(13)	177.4(3)	Os(1)–Os(8)–Os(5)	88.2(2)
Os(9)–Os(2)–Os(12)	60.5(2)	Os(10)–Os(2)–Os(12)	60.0(2)	Os(1)–Os(8)–Os(7)	59.2(2)	Os(5)–Os(8)–Os(7)	59.2(2)
Os(9)–Os(2)–Os(14)	179.3(2)	Os(10)–Os(2)–Os(14)	59.6(2)	Os(1)–Os(8)–Os(10)	59.8(2)	Os(5)–Os(8)–Os(10)	57.8(2)
Os(12)–Os(2)–Os(14)	119.4(2)	Os(9)–Os(2)–Os(16)	120.1(2)	Os(7)–Os(8)–Os(10)	88.4(2)	Os(1)–Os(8)–Os(12)	120.7(2)
Os(10)–Os(2)–Os(16)	58.0(2)	Os(12)–Os(2)–Os(16)	89.6(2)	Os(5)–Os(8)–Os(12)	60.0(2)	Os(7)–Os(8)–Os(12)	119.2(2)
Os(14)–Os(2)–Os(16)	60.6(2)	Os(9)–Os(2)–Os(19)	60.2(2)	Os(10)–Os(8)–Os(12)	60.9(2)	Os(1)–Os(8)–Os(13)	59.9(2)
Os(10)–Os(2)–Os(19)	89.1(2)	Os(12)–Os(2)–Os(19)	60.6(2)	Os(5)–Os(8)–Os(13)	119.2(2)	Os(7)–Os(8)–Os(13)	60.0(2)
Os(14)–Os(2)–Os(19)	120.5(2)	Os(16)–Os(2)–Os(19)	59.9(2)	Os(10)–Os(8)–Os(13)	119.6(2)	Os(12)–Os(8)–Os(13)	178.8(2)
Os(1)–Os(3)–Os(4)	60.2(2)	Os(1)–Os(3)–Os(5)	91.0(2)	Os(2)–Os(9)–Os(12)	59.0(2)	Os(2)–Os(9)–Os(19)	59.6(2)
Os(4)–Os(3)–Os(5)	121.9(3)	Os(1)–Os(3)–Os(7)	59.3(2)	Os(12)–Os(9)–Os(19)	59.9(2)	Os(1)–Os(10)–Os(2)	178.5(2)
Os(4)–Os(3)–Os(7)	119.5(2)	Os(5)–Os(3)–Os(7)	60.0(2)	Os(1)–Os(10)–Os(3)	61.1(2)	Os(2)–Os(10)–Os(3)	120.1(2)
Os(1)–Os(3)–Os(10)	61.1(2)	Os(4)–Os(3)–Os(10)	62.0(2)	Os(1)–Os(10)–Os(4)	59.6(2)	Os(2)–Os(10)–Os(4)	120.0(2)
Os(5)–Os(3)–Os(10)	59.9(2)	Os(7)–Os(3)–Os(10)	89.2(2)	Os(3)–Os(10)–Os(4)	60.2(2)	Os(1)–Os(10)–Os(5)	91.4(2)
Os(1)–Os(3)–Os(11)	118.9(2)	Os(4)–Os(3)–Os(11)	176.3(3)	Os(2)–Os(10)–Os(5)	90.0(2)	Os(3)–Os(10)–Os(5)	60.5(2)
Os(5)–Os(3)–Os(11)	61.2(2)	Os(7)–Os(3)–Os(11)	59.7(2)	Os(4)–Os(10)–Os(5)	120.7(2)	Os(1)–Os(10)–Os(8)	61.1(2)
Os(10)–Os(3)–Os(11)	121.0(2)	Os(1)–Os(3)–Os(16)	121.6(3)	Os(2)–Os(10)–Os(8)	119.1(2)	Os(3)–Os(10)–Os(8)	92.7(2)
Os(4)–Os(3)–Os(16)	91.8(2)	Os(5)–Os(3)–Os(16)	60.0(2)	Os(4)–Os(10)–Os(8)	120.8(2)	Os(5)–Os(10)–Os(8)	62.0(2)
Os(7)–Os(3)–Os(16)	120.0(2)	Os(10)–Os(3)–Os(16)	60.5(2)	Os(1)–Os(10)–Os(12)	120.9(2)	Os(2)–Os(10)–Os(12)	59.4(2)
Os(11)–Os(3)–Os(16)	91.6(2)	Os(1)–Os(3)–Os(17)	176.5(3)	Os(3)–Os(10)–Os(12)	121.4(2)	Os(4)–Os(10)–Os(12)	178.4(2)
Os(4)–Os(3)–Os(17)	119.7(2)	Os(5)–Os(3)–Os(17)	91.8(2)	Os(5)–Os(10)–Os(12)	61.0(2)	Os(8)–Os(10)–Os(12)	59.7(2)
Os(7)–Os(3)–Os(17)	120.6(2)	Os(10)–Os(3)–Os(17)	122.2(2)	Os(1)–Os(10)–Os(14)	120.1(2)	Os(2)–Os(10)–Os(14)	59.4(2)
Os(11)–Os(3)–Os(17)	60.9(2)	Os(16)–Os(3)–Os(17)	61.7(2)	Os(3)–Os(10)–Os(14)	91.4(2)	Os(4)–Os(10)–Os(14)	60.6(2)
Os(1)–Os(3)–Os(20)	120.7(2)	Os(4)–Os(3)–Os(20)	60.4(2)	Os(5)–Os(10)–Os(14)	121.4(2)	Os(8)–Os(10)–Os(14)	175.7(3)
Os(5)–Os(3)–Os(20)	120.1(2)	Os(7)–Os(3)–Os(20)	180.0(5)	Os(12)–Os(10)–Os(14)	118.8(2)	Os(1)–Os(10)–Os(16)	121.0(3)
Os(10)–Os(3)–Os(20)	90.9(2)	Os(11)–Os(3)–Os(20)	120.4(2)	Os(2)–Os(10)–Os(16)	60.2(2)	Os(3)–Os(10)–Os(16)	59.9(2)
Os(16)–Os(3)–Os(20)	60.1(2)	Os(17)–Os(3)–Os(20)	59.4(2)	Os(4)–Os(10)–Os(16)	90.4(2)	Os(5)–Os(10)–Os(16)	60.0(2)
Os(1)–Os(4)–Os(3)	60.3(2)	Os(1)–Os(4)–Os(6)	177.6(3)	Os(8)–Os(10)–Os(16)	122.0(2)	Os(12)–Os(10)–Os(16)	90.6(2)
Os(3)–Os(4)–Os(6)	121.4(2)	Os(1)–Os(4)–Os(10)	59.7(2)	Os(14)–Os(10)–Os(16)	61.3(2)	Os(3)–Os(11)–Os(5)	58.2(2)
Os(3)–Os(4)–Os(10)	57.8(2)	Os(6)–Os(4)–Os(10)	119.4(2)	Os(3)–Os(11)–Os(7)	60.8(2)	Os(5)–Os(11)–Os(7)	59.4(2)
Os(1)–Os(4)–Os(14)	118.9(2)	Os(3)–Os(4)–Os(14)	89.1(2)	Os(3)–Os(11)–Os(15)	120.1(2)	Os(5)–Os(11)–Os(15)	120.0(2)
Os(6)–Os(4)–Os(14)	60.2(2)	Os(10)–Os(4)–Os(14)	59.2(2)	Os(7)–Os(11)–Os(15)	178.6(2)	Os(3)–Os(11)–Os(17)	59.7(2)
Os(1)–Os(4)–Os(20)	121.1(2)	Os(3)–Os(4)–Os(20)	60.8(2)	Os(5)–Os(11)–Os(17)	89.3(2)	Os(7)–Os(11)–Os(17)	120.6(2)
Os(6)–Os(4)–Os(20)	60.7(2)	Os(10)–Os(4)–Os(20)	88.7(2)	Os(15)–Os(11)–Os(17)	60.4(2)	Os(3)–Os(11)–Os(18)	88.8(2)
Os(14)–Os(4)–Os(20)	59.8(2)	Os(3)–Os(5)–Os(7)	61.9(2)	Os(5)–Os(11)–Os(18)	60.2(2)	Os(7)–Os(11)–Os(18)	119.6(2)
Os(3)–Os(5)–Os(8)	91.2(2)	Os(7)–Os(5)–Os(8)	59.8(2)	Os(15)–Os(11)–Os(18)	59.9(2)	Os(17)–Os(11)–Os(18)	59.7(2)
Os(3)–Os(5)–Os(10)	59.7(2)	Os(7)–Os(5)–Os(10)	90.1(2)	Os(2)–Os(12)–Os(5)	88.7(2)	Os(2)–Os(12)–Os(8)	120.0(2)
Os(8)–Os(5)–Os(10)	60.2(2)	Os(3)–Os(5)–Os(11)	60.6(2)	Os(5)–Os(12)–Os(8)	60.7(2)	Os(2)–Os(12)–Os(9)	60.5(2)
Os(7)–Os(5)–Os(11)	60.1(2)	Os(8)–Os(5)–Os(11)	119.9(2)	Os(5)–Os(12)–Os(9)	119.3(2)	Os(8)–Os(12)–Os(9)	179.5(2)
Os(10)–Os(5)–Os(11)	120.2(2)	Os(3)–Os(5)–Os(12)	121.1(2)	Os(2)–Os(12)–Os(10)	60.6(2)	Os(5)–Os(12)–Os(10)	57.6(2)
Os(7)–Os(5)–Os(12)	119.1(2)	Os(8)–Os(5)–Os(12)	59.3(2)	Os(8)–Os(12)–Os(10)	59.4(2)	Os(9)–Os(12)–Os(10)	121.1(2)
Os(10)–Os(5)–Os(12)	61.4(2)	Os(11)–Os(5) Os(12)	177.8(2)	Os(2)–Os(12)–Os(19)	60.1(2)	Os(5)–Os(12)–Os(19)	59.3(2)
Os(3)–Os(5)–Os(16)	59.8(2)	Os(7)–Os(5)–Os(16)	121.6(2)	Os(8)–Os(12)–Os(19)	120.0(2)	Os(9)–Os(12)–Os(19)	60.0(2)
Os(8)–Os(5)–Os(16)	120.5(2)	Os(10)–Os(5)–Os(16)	60.3(2)	Os(10)–Os(12)–Os(19)	89.2(2)	Os(1)–Os(13)–Os(7)	58.9(2)
Os(11)–Os(5)–Os(16)	91.1(2)	Os(12)–Os(5)–Os(16)	91.0(2)	Os(1)–Os(13)–Os(8)	59.8(2)	Os(7)–Os(13)–Os(8)	59.0(2)
Os(3)–Os(5)–Os(18)	90.0(2)	Os(7)–Os(5)–Os(18)	120.0(2)	Os(2)–Os(14)–Os(4)	121.2(2)	Os(2)–Os(14)–Os(6)	178.6(2)
Os(8)–Os(5)–Os(18)	178.4(2)	Os(10)–Os(5)–Os(18)	121.3(2)	Os(4)–Os(14)–Os(6)	59.7(2)	Os(2)–Os(14)–Os(10)	61.0(2)
Os(11)–Os(5)–Os(18)	60.0(2)	Os(12)–Os(5)–Os(18)	120.8(2)	Os(4)–Os(14)–Os(10)	60.2(2)	Os(6)–Os(14)–Os(10)	119.9(2)
Os(16)–Os(5)–Os(18)	61.0(2)	Os(3)–Os(5)–Os(19)	120.9(2)	Os(2)–Os(14)–Os(16)	59.7(2)	Os(4)–Os(14)–Os(16)	88.4(2)
Os(7)–Os(5)–Os(19)	176.9(2)	Os(8)–Os(5)–Os(19)	120.3(2)	Os(6)–Os(14)–Os(16)	119.6(2)	Os(10)–Os(14)–Os(16)	58.2(2)
Os(10)–Os(5)–Os(19)	92.5(2)	Os(11)–Os(5)–Os(19)	119.7(2)	Os(2)–Os(14)–Os(20)	118.7(2)	Os(4)–Os(14)–Os(20)	59.9(2)
Os(12)–Os(5)–Os(19)	61.0(2)	Os(16)–Os(5)–Os(19)	61.2(2)	Os(6)–Os(14)–Os(20)	60.6(2)	Os(10)–Os(14)–Os(20)	89.3(2)
Os(18)–Os(5)–Os(19)	59.7(2)	Os(4)–Os(6)–Os(14)	60.1(2)	Os(16)–Os(14)–Os(20)	59.1(2)	Os(11)–Os(15)–Os(17)	59.9(2)
Os(4)–Os(6)–Os(20)	59.6(2)	Os(14)–Os(6)–Os(20)	59.4(2)	Os(11)–Os(15)–Os(18)	59.7(2)	Os(17)–Os(15)–Os(18)	59.5(2)

Table 2 (*continued*)

Os(2)–Os(16)–Os(3)	121.4(2)	Os(2)–Os(16)–Os(5)	90.7(2)	Os(15)–Os(17)–Os(20)	178.6(3)	Os(16)–Os(17)–Os(20)	59.2(2)
Os(3)–Os(16)–Os(5)	60.2(2)	Os(2)–Os(16)–Os(10)	61.8(2)	Os(18)–Os(17)–Os(20)	119.0(2)	Os(5)–Os(18)–Os(11)	59.9(2)
Os(3)–Os(16)–Os(10)	59.6(2)	Os(5)–Os(16)–Os(10)	59.6(2)	Os(5)–Os(18)–Os(15)	120.3(2)	Os(11)–Os(18)–Os(15)	60.4(2)
Os(2)–Os(16)–Os(14)	59.7(2)	Os(3)–Os(16)–Os(14)	90.7(2)	Os(5)–Os(18)–Os(16)	57.8(2)	Os(11)–Os(18)–Os(16)	89.1(2)
Os(5)–Os(16)–Os(14)	120.1(2)	Os(10)–Os(16)–Os(14)	60.5(2)	Os(15)–Os(18)–Os(16)	121.3(2)	Os(5)–Os(18)–Os(17)	89.6(2)
Os(2)–Os(16)–Os(17)	177.7(2)	Os(3)–Os(16)–Os(17)	60.7(2)	Os(11)–Os(18)–Os(17)	60.6(2)	Os(15)–Os(18)–Os(17)	60.9(2)
Os(5)–Os(16)–Os(17)	91.3(2)	Os(10)–Os(16)–Os(17)	120.3(2)	Os(16)–Os(18)–Os(17)	60.4(2)	Os(5)–Os(18)–Os(19)	59.7(2)
Os(14)–Os(16)–Os(17)	120.1(2)	Os(2)–Os(16)–Os(18)	120.3(2)	Os(11)–Os(18)–Os(19)	119.5(2)	Os(15)–Os(18)–Os(19)	178.5(2)
Os(3)–Os(16)–Os(18)	90.4(2)	Os(5)–Os(16)–Os(18)	61.2(2)	Os(16)–Os(18)–Os(19)	60.1(2)	Os(17)–Os(18)–Os(19)	120.4(2)
Os(10)–Os(16)–Os(18)	120.8(2)	Os(14)–Os(16)–Os(18)	178.6(2)	Os(2)–Os(19)–Os(9)	60.2(2)	Os(5)–Os(19)–Os(9)	119.7(2)
Os(17)–Os(16)–Os(18)	59.8(2)	Os(2)–Os(16)–Os(19)	60.7(2)	Os(2)–Os(19)–Os(12)	59.2(2)	Os(5)–Os(19)–Os(12)	59.7(2)
Os(3)–Os(16)–Os(19)	120.9(2)	Os(5)–Os(16)–Os(19)	60.7(2)	Os(9)–Os(19)–Os(12)	60.0(2)	Os(2)–Os(19)–Os(16)	59.4(2)
Os(10)–Os(16)–Os(19)	91.7(2)	Os(14)–Os(16)–Os(19)	120.4(2)	Os(5)–Os(19)–Os(16)	58.1(2)	Os(9)–Os(19)–Os(16)	119.6(2)
Os(17)–Os(16)–Os(19)	119.4(2)	Os(18)–Os(16)–Os(19)	59.6(2)	Os(12)–Os(19)–Os(16)	88.5(2)	Os(2)–Os(19)–Os(18)	119.7(2)
Os(2)–Os(16)–Os(20)	120.0(2)	Os(3)–Os(16)–Os(20)	62.0(2)	Os(5)–Os(19)–Os(18)	60.6(2)	Os(9)–Os(19)–Os(18)	179.6(2)
Os(5)–Os(16)–Os(20)	122.3(3)	Os(10)–Os(16)–Os(20)	91.5(2)	Os(12)–Os(19)–Os(18)	120.3(2)	Os(16)–Os(19)–Os(18)	60.3(2)
Os(14)–Os(16)–Os(20)	60.4(2)	Os(17)–Os(16)–Os(20)	59.7(2)	Os(3)–Os(20)–Os(4)	58.8(2)	Os(3)–Os(20)–Os(6)	118.5(2)
Os(18)–Os(16)–Os(20)	119.5(2)	Os(19)–Os(16)–Os(20)	176.5(2)	Os(4)–Os(20)–Os(6)	59.7(2)	Os(3)–Os(20)–Os(14)	88.4(2)
Os(3)–Os(17)–Os(11)	59.3(2)	Os(3)–Os(17)–Os(15)	119.0(2)	Os(4)–Os(20)–Os(14)	60.4(2)	Os(6)–Os(20)–Os(14)	60.0(2)
Os(11)–Os(17)–Os(15)	59.7(2)	Os(3)–Os(17)–Os(16)	57.6(2)	Os(3)–Os(20)–Os(16)	57.8(2)	Os(4)–Os(20)–Os(16)	89.4(2)
Os(11)–Os(17)–Os(16)	88.3(2)	Os(15)–Os(17)–Os(16)	119.4(2)	Os(6)–Os(20)–Os(16)	120.5(2)	Os(14)–Os(20)–Os(16)	60.5(2)
Os(3)–Os(17)–Os(18)	88.6(2)	Os(11)–Os(17)–Os(18)	59.7(2)	Os(3)–Os(20)–Os(17)	59.8(2)	Os(4)–Os(20)–Os(17)	118.5(2)
Os(15)–Os(17)–Os(18)	59.6(2)	Os(16)–Os(17)–Os(18)	59.8(2)	Os(6)–Os(20)–Os(17)	177.0(3)	Os(14)–Os(20)–Os(17)	121.5(2)
Os(3)–Os(17)–Os(20)	60.8(2)	Os(11)–Os(17)–Os(20)	120.1(2)	Os(16)–Os(20)–Os(17)	61.1(2)		

at temperatures between 260 and 300 °C and initial pressures of around 10^{-3} Torr. From the negative-ion FAB mass spectrum of the $[PBu^n_4]^+$ salt of the carbonyl anion the formulation of the cluster **3** as either $[Os_{20}(CO)_{40}]^{2-}$ or $[Os_{20}C(CO)_{40}]^{2-}$ (dianion, *m/z* 2467; monoanion, *m/z* 4937; dianion + $PBu^n_4{}^+$, *m/z* 5197) was deduced, while the simplicity of the ν(CO) absorption band pattern (see Experimental section) in the infrared spectrum of the compound indicated a highly symmetrical cluster geometry. The formulation inferred from the mass spectrum of **3** along with the similarity of the IR band pattern to that of **1** led to the proposal that **3** was the higher homologue of **1**, *i.e.* a cubic close-packed tetrahedron of 20 metal atoms enveloped by a ligand shell of 40 end-on bonded carbonyls.

This was confirmed by the single-crystal structure analysis of its $[PBu^n_4]^+$ salt which has established a hitherto unobserved metal-core geometry. The molecular structure of the cluster dianion is depicted in Fig. 3(*a*), the bare Os_{20} metal core in Fig. 3(*b*), while the principal bond distances and interbond angles are listed in Table 2. The metal polyhedron may be derived from that of $[Os_{10}X(CO)_{24}]^{2-}$ (X = H_4 or C) by addition of a further planar triangular layer of 10 osmium atoms. This kind of skeletal geometry has been the object of a number of theoretical studies related to the abundant M_{20} clusters detected in supersonic beams of alkali-metal vapours.[15]

Neither the crystal structure analysis nor IR, ^1H and ^{13}C NMR spectroscopy (see below) has revealed the presence of interstitial atoms (C or H) in the four octahedral or eleven tetrahedral cavities of the core. It should, however, be pointed out that a four-fold disorder of a carbido ligand between the symmetry-related octahedral cavities of the cluster would make a carbon atom virtually invisible in the crystal structure determination and would also obscure any possible secondary effects on the metal framework. Moreover, for a molecular mass of this magnitude, the FAB mass spectra obtained are not unambiguous in determining the presence or absence of interstitial or surface-located hydrogen or even carbon atoms. In the light of the accumulated negative evidence for such additional ligands the formulation of **3** as $[Os_{20}(CO)_{40}]^{2-}$ is considered to be the most appropriate, even though the c.v.e. count based on this formula is lower than that predicted by a number of electron-counting rules (see below).

The mean metal–metal distances within the cluster framework [*d*(Os–Os) = 2.786, 2.747, 2.678 Å respectively for the Os atoms surrounding the three different types of tetrahedral cavities and 2.746 Å for the octahedral cavities] are similar to those of **2** which also lacks interstitial atoms. The four osmium atoms of the unique tetrahedron at the centre of the cluster [Os(3), Os(5), Os(10) and Os(16)] have the highest metal–metal connectivity (nine) and an average bond distance of 2.678(8) Å, again similar to that of the bulk metal (2.6754 Å).[10]

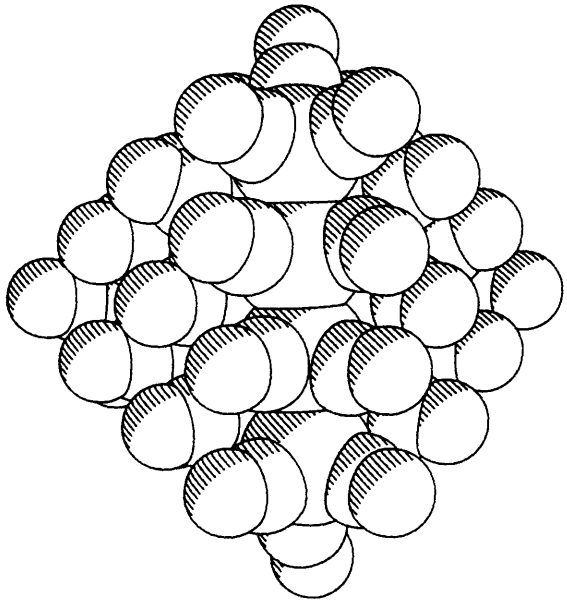

Fig. 4 Computed space-filling model of cluster **3** showing the high symmetry of the CO ligand shell

The symmetry of the core is matched by that of the CO ligand shell in which there are 40 terminal carbonyl ligands in three chemically distinct environments. The packing of the carbonyls is illustrated in the computed space-filling model of the cluster in Fig. 4. The co-ordination of CO to the cluster surface may be compared to that observed for chemisorbed carbon monoxide on the (111) surface of cubic close-packed metals. Another structural feature of the ligand shell of many high-nuclearity clusters is the reduced steric interaction between the carbonyls in comparison to the situation found in low-nuclearity species.

The application of a surface force-field model developed for polynuclear metal carbonyls[16] to the ligand interactions in cluster **3** has established a steric repulsion energy per carbonyl ligand ($E_{steric} = E_{tot}/n_{CO}$; E_{tot} is the sum of the bond-stretch energy, M–CO angle energy, van der Waals energy and electrostatic energy of the carbonyls on the metal surface and n_{CO} is the number of CO groups in the cluster) which is only half of that in a D_{3h} $M_3(CO)_{12}$ cluster and *ca.* 10% of that found for mononuclear metal hexacarbonyls. This decreased ligand repulsion may be viewed as representing an intermediate case between the situation in molecular metal carbonyls and that found on CO-monolayered metal surfaces.

It proved particularly difficult to obtain a clean ^{13}C NMR spectrum of cluster **3** since most spectra recorded were obscured by sets of paramagnetically shifted resonances ($150 < \delta < 320$) which differed in appearance and chemical shift depending on the 'history' of the sample and the solvent used. The only signals in the typical ^{13}CO range common to all spectra were the resonances at δ 158.0, 179.5 and 179.8 with an approximate intensity ratio of 3:1:6 (=12 CO:4 CO:24 CO). This is consistent with three chemically distinct CO environments in **3** as formulated above. There was no indication of a carbide resonance in the chemical shift range between δ 350 and 480 which was additionally supported by the absence of a ν(carbide) band in the IR spectrum between 500 and 850 cm^{-1}.

The most characteristic feature of the chemical reactivity of both clusters **2** and **3** is their complicated redox behaviour. This has so far prohibited their use as building blocks in cluster condensation reactions with metal electrophiles. However, systematic chemical oxidation of **3** with $[Fe(cp)_2]BF_4$ (cp = η^5-C_5H_5) and reduction with $[Co(cp)_2]$ has established the existence of at least five thermally stable oxidation states of the cluster which have been characterised by IR spectroscopy (Table 3). It should be pointed out that the ν(CO) band pattern, while being shifted as a consequence of a change in the cluster charge, remains essentially unchanged in all of the five species described here. This implies the retention of the overall cluster structure in these oxidation states. The main structural implication of these conversions is therefore most probably a mere 'breathing' (*i.e.* expansion and contraction of the metal core), and the facile interconvertibility of the different redox states provides additional support for this proposition. A remarkable chemical consequence is the almost instantaneous conproportionation reactions of **3** which occur whenever two species which differ by an overall molecular charge of two or more are present in solution [equations (1) and (2)]. A solution

$$[Os_{20}(CO)_{40}]^{n-} + [Os_{20}(CO)_{40}]^{(n+2)-} \longrightarrow 2\,[Os_{20}(CO)_{40}]^{(n+1)-} \quad (1)$$

$$[Os_{20}(CO)_{40}]^{n-} + [Os_{20}(CO)_{40}]^{(n+3)-} \longrightarrow [Os_{20}(CO)_{40}]^{(n+1)-} + [Os_{20}(CO)_{40}]^{(n+2)-}$$

$$\downarrow + [Os_{20}(CO)_{40}]^{n-}$$

$$3\,[Os_{20}(CO)_{40}]^{(n+1)-} \quad (2)$$

Table 3 Infrared data of the five characterised oxidation states of cluster **3**

Compound	$\tilde{\nu}$(CO)/cm^{-1}
$[Os_{20}(CO)_{40}]$	2074s, 2036s[a]
$[Os_{20}(CO)_{40}]^-$	2059s, 2016s[a]
$[Os_{20}(CO)_{40}]^{2-}$	2041s, 2003s, 1957w[b]
$[Os_{20}(CO)_{40}]^{3-}$	2030s, 1992s, 1943w[b]
$[Os_{20}(CO)_{40}]^{4-}$	2017s, 1968s[b]

[a] In CH_2Cl_2. [b] In tetrahydrofuran (thf).

of the anionic cluster **3** in one of the five chemically accessible redox states may therefore be 'titrated' with the same compound in a different redox state to give a quantitative conversion into an intermediate redox state. Electrochemical studies of both **2** and **3** have revealed an even larger number of accessible redox states for both clusters. The results of these investigations will be published elsewhere.[17]

The tetrahedral metal core of a cubic close-packed M_{20} cluster (M = late transition metal) has been postulated for some time. Lauher[18] predicted a c.v.e. count of 254 for such a species while Teo and Sloane[19] deduced a topological electron count of 252. Assuming the absence of any further light atoms in the structure of **3**, based on the experimental evidence presented above, the formulation as $[Os_{20}(CO)_{40}]^{2-}$ corresponds to an electron count of 242, thus substantially less than predicted. A rationale for this situation has recently been given by Lauher.[20] The starting point in Lauher's approach is the bare metal cluster which has a certain number of cluster valence molecular orbitals (CVMOs) which can either act as ligand-acceptor orbitals or are non-bonding containing the electrons associated with the metal atoms themselves.[21] This involves MOs which are *n*s, *n*p as well as (*n* − 1)d (*n* = principal quantum number of the valence shell of the atoms involved) in character, of which all the d-type orbitals are used in metal–metal or metal–ligand bonding. The CVMOs calculated for the bare transition-metal cluster are used as frontier orbitals for the interaction with the group orbitals of the ligand shell as a whole. For bonding interactions, a significant overlap between the CVMOs and the ligand orbitals is required, a condition which is fulfilled for most 'convex' metal frameworks. In the cluster dianion **3** a special situation arises which so far had not to be considered in the high-nuclearity cluster chemistry of osmium. The Os(3), Os(5), Os(10) and Os(16) atoms in Fig. 3(*b*) lie at the centre of the four faces of the tetrahedron, thus resembling atoms on an extended metal surface. For all four osmium atoms there will be in-plane metal–metal bonding and antibonding interactions with the appropriate orbitals of the neighbouring atoms. These orbitals have mainly d character and there are two d-type orbitals per face-centring metal atom involved. Since the antibonding orbitals are essentially in-plane they cannot act as ligand-acceptor orbitals and therefore lie at relatively high energy in the frontier-orbital region. As a consequence, they may not all be populated in the most stable electronic state of the cluster which would account for the apparent electron deficiency of **3**. If electrons were added to or removed from **3** these orbitals would be filled or depopulated, and since they are essentially in-plane metal–metal antibonding the structural changes associated with this process would amount to a mere 'breathing', *i.e.* uniform expansion or contraction, of the metal framework while the overall symmetry is retained, as is inferred from the spectroscopic data in Table 3. Lauher's model retains its validity even if hitherto undetected interstitial or surface-located ligands were present, the only difference being the degree to which the frontier orbitals are populated. It is anticipated that on increasing the nuclearity of clusters the density of frontier orbitals which are primarily metal–metal non- or anti-bonding in character increases dramatically. This would explain the increased redox activity predicted, and observed, for these systems. High-nuclearity clusters may thus play a role as effective electron reservoirs which deserve a more detailed theoretical as well as experimental investigation in the future.

The isolation and characterisation of cluster **3** and its homologous relationship to **1** has again raised the question of the preferred cluster geometries and nuclearities generated under the thermodynamically controlled conditions of most pyrolysis reactions performed at high temperatures (> 200 °C) involving osmium carbonyl derivatives. In these thermolyses, certain nuclearities are found to dominate the product distributions, thereby allowing highly selective syntheses of some species (*e.g.* **1**) under the appropriate reaction conditions while

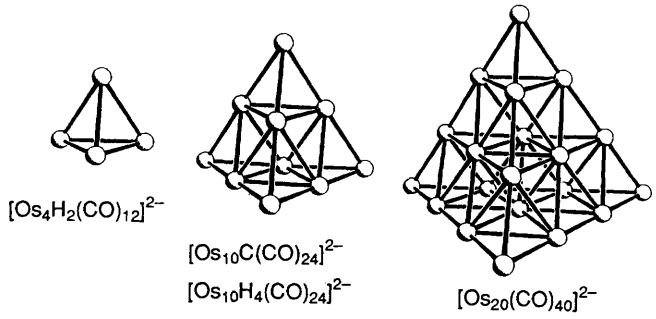

Fig. 5 The series of structurally characterised tetrahedral osmium cluster dianions

others appear only as minor fractions. For osmium clusters, the generation of metal cores containing 4, 6, 10 and 20 metal atoms appears to be particularly favoured. With the exception of the hexaosmium clusters, these nuclearities correspond to the series of 'magic numbers' 4, 10, 20, ... associated with molecular tetrahedra of edge lengths two (atoms), three and four and therefore represent the gradual build-up of cubic close-packed cores of tetrahedral symmetry (Fig. 5). It remains to be seen whether further 'islands of stability' are represented by tetrahedral cluster geometries, the next in line being $[Os_{35}(CO)_{60}]^{x-}$, $[Os_{56}(CO)_{84}]^{y-}$, *etc.*

Conclusion

The two cluster dianions **2** and **3** are by far the largest osmium carbonyl clusters characterised to date. Their chemical properties, in particular their redox behaviour, sets them apart from anything observed previously in the cluster chemistry of osmium. The principal problems to be encountered on going to even higher nuclearities will be the increase in redox activity and, consequently, reduced chemical stability of the materials isolated, the decrease of solubility in practically all solvent systems, as well as the limits set by X-ray crystallography with Mo-Kα radiation (size of the unit cell, X-ray absorption by the heavy atoms) and by the established purification techniques (chromatography, fractional extraction and crystallisation). It is likely that very large metal carbonyl clusters are formed in many of the common synthetic procedures and that the difficulties encountered in the isolation and characterisation of the compounds have restricted their detection. To overcome these inhibiting factors will remain a challenge in the chemistry of high-nuclearity clusters.

Experimental

Vacuum pyrolyses were typically carried out in flame-dried Carius tubes (180 cm^3). These were sealed under vacuum, placed into stainless-steel liners and heated in an oven at controlled temperature for the required time. Pyrolysis tubes were opened behind an explosion-proof shield. The reaction mixtures obtained were separated by thin-layer chromatography on 20 × 20 cm glass plates coated with a 0.25 or 1 mm layer of Merck Kieselgel $60F_{254}$.

All manipulations involving clusters **2** or **3** after their initial isolation were performed under an inert-gas atmosphere of argon (purity 99.997%) in standard (Schlenk) glassware. Solvents and solutions were transferred from one reaction vessel to another with the aid of stainless-steel canulae under complete exclusion of air and moisture ('canula/septa technique'). The solvents were dried according to standard procedures and saturated with Ar or N_2 before use. The compound $[Os_3(CO)_{10}(NCMe)_2]$ was prepared according to the literature procedure.[22] All other chemicals were used as purchased without further purification. The ^{13}C-enriched samples used for the ^{13}C NMR studies were synthesised from ^{13}C-enriched $[Os_3(CO)_{12}]$.[23]

Solution infrared spectra were recorded in NaCl or CaF_2 cells (path length 0.5 mm) on a Perkin-Elmer PE983 or 1710 FT spectrometer. Fast-atom bombardment (FAB) mass spectra of the ionic clusters were obtained on a Kratos MS50 spectrometer. The matrix used was either 3-nitrobenzyl alcohol or thioglycerol and the calibrant CsI. Simulations of the isotopic distributions of the parent ions were carried out with a computer program implemented on the DS90 data system of a Kratos MS890 mass spectrometer. The ^1H and ^{13}C NMR spectra were recorded on a Bruker AM400 spectrometer equipped with a B-VT-1000 variable-temperature unit.

Synthesis of $[N(PPh_3)_2]_2[Os_{17}(CO)_{36}]$ **2** *and* $[N(PPh_3)_2]_2[Os_{20}(CO)_{40}]$ **3** *by Vacuum Pyrolysis of* $[Os_3(CO)_{10}(NCMe)_2]$.—A Carius tube (180 cm^3) was filled with a suspension of $[Os_3(CO)_{10}(NCMe)_2]$ (1 g) in CH_2Cl_2 (30 cm^3). The solvent was evaporated under reduced pressure and the solid evenly distributed over the interior surface of the tube which was sealed at 10^{-3} Torr. The precursor compound was pyrolysed at 300 °C for 70 h to yield a brown-black powder which was initially sparingly soluble in acetone. Heating under reflux in a mixture of acetone (100 cm^3) and methanol (30 cm^3) in the presence of $[N(PPh_3)_2]Cl$ (1.2 g) for 20 h resulted in almost complete dissolution of the solid. The deep brown solution was filtered (*ca.* 100 mg insoluble material) and the filtrate evaporated to dryness. After the removal of surplus $[N(PPh_3)_2]Cl$ by extraction with methanol, the residue was dissolved in acetone (25 cm^3) and separated by thin-layer chromatography (silica gel) using acetone–hexane (60:40) as eluent. Apart from the neutral low-nuclearity fractions moving near the solvent front (R_f = 0.9, *ca.* 100 mg of Os_4 and Os_5 clusters), the major fractions were as follows.

$[N(PPh_3)_2]_2[Os_{17}(CO)_{36}]$ **2**: R_f = 0.65, brown, 73 mg (7%). IR (CH_2Cl_2): ν(CO) 2086vw, 2060s, 2044vs, 2040vs, 2028m, 2000m, 1987m and 1969w cm^{-1}. NMR (CD_2Cl_2): ^1H, δ 7.5 – 7.9 [m, $N(PPh_3)_2^+$]; ^{13}C, δ 196.8 (6 CO), 195.1 (3 CO), 192.6 (3 CO), 187.2 (9 CO), 179.9 (9 CO), 173.4 (3 CO) and 166.5 (3 CO). Negative-ion FAB mass spectrum (most abundant isotopomers): *m/z* (dianion) 2121 (simulated: 2122), (monoanion) 4243 (simulated: 4244).

$[N(PPh_3)_2]_2[Os_{10}C(CO)_{24}]$ **1**: R_f = 0.60, red, 350 mg (29%).[9]

$[N(PPh_3)_2]_2[Os_{20}(CO)_{40}]$ **3**: R_f = 0.40, brown-green, 200 mg (20%). IR (CH_2Cl_2): ν(CO) 2045s, 2002s and 1955w cm^{-1}; no bands for an interstitial carbide observed between 500 and 850 cm^{-1} (NMe_4^+ salt, CsI disc). ^{13}C NMR [$(CD_3)_2CO$, 295 K]: δ 158.0 (12 CO), 179.5 (4 CO) and 179.8 (24 CO); no carbide resonance between δ 350 and 480. Negative-ion FAB mass spectrum of the anion (most abundant isotopomers): *m/z* (dianion) 2467 (simulated: 2464), (monoanion) 4937 (simulated: 4929), other minor fractions, including the baseline, accounted for *ca.* 100 mg of material.

The $[AsPh_4]^+$ salt of cluster **2** and $[PBu^n_4]^+$ salt of **3** were obtained by cation metathesis with $[AsPh_4]Cl$ and $[PBu^n_4]Cl$, respectively, and crystallised by slow evaporation of solutions of the salts in acetone–methanol (2:1) for **2** and acetone–ethanol (1:1) for **3**.

Systematic Chemical Oxidation of Cluster **3**.—A solution of $[N(PPh_3)_2]_2[Os_{20}(CO)_{40}]$ **3** (30 mg, 5 × 10^{-6} mol in 15 cm^3 CH_2Cl_2) was titrated with a solution of $[Fe(\eta^5\text{-}C_5H_5)_2]BF_4$ (10 mg, 36.6 × 10^{-6} mol in 10 cm^3 CH_2Cl_2). The progress of the redox reaction was monitored by infrared spectroscopy which initially indicated the formation of the monoanionic cluster (complete after addition of *ca.* 1.4 cm^3). IR (CH_2Cl_2): 2059s and 2016s cm^{-1}. Negative-ion FAB mass spectrum: most abundant isotopomer of the cluster monoanionum at *m/z* 4933. After addition of a further equivalent of $[Fe(\eta^5\text{-}C_5H_5)_2]BF_4$, **3** was converted into its neutral form. IR (CH_2Cl_2): 2074s and 2036s cm^{-1}. After prolonged stirring of either oxidation product in the air both compounds were slowly reconverted into the salt

of the cluster dianion which had identical IR and mass spectroscopic properties to those of the starting material.

Systematic Chemical Reduction of Cluster **3**.—A solution of $[N(PPh_3)_2]_2[Os_{20}(CO)_{40}]$ **3** (30 mg, 5×10^{-6} mol in 15 cm^3 thf) was titrated with a solution of $[Co(\eta^5\text{-}C_5H_5)_2]$ (10 mg, 52.9×10^{-6} mol in 10 cm^3 thf). The progress of the redox reaction was monitored by infrared spectroscopy which initially indicated the formation of the trianionic cluster (complete after addition of *ca.* 1.0 cm^3). IR (CH_2Cl_2 or thf): 2030s, 1992s and 1943w cm^{-1}. Negative-ion FAB mass spectrum (most abundant isotopomer): *m/z* (dianion) 2469, (monoanion) 4934. After addition of a further equivalent of $[Co(\eta^5\text{-}C_5H_5)_2]$, **3** was converted into its tetraanionic form. IR (CH_2Cl_2 or thf): 2017s and 1968s cm^{-1}. After prolonged stirring of either reduction product in the air both compounds were rapidly reconverted into the salt of the cluster dianion which had identical IR and mass spectroscopic properties to those of the starting material.

Conproportionation of $[N(PPh_3)_2]_4[Os_{20}(CO)_{40}]$ *and* $[N(PPh_3)_2]_2[Os_{20}(CO)_{40}]$ *to yield* $[N(PPh_3)_2]_3[Os_{20}(CO)_{40}]$.—A solution of $[N(PPh_3)_2]_4[Os_{20}(CO)_{40}]$ in thf {+20 mg $[N(PPh_3)_2]Cl$} prepared as described above was added dropwise to a solution of $[N(PPh_3)_2]_2[Os_{20}(CO)_{40}]$ (30 mg, 5×10^{-6} mol in 15 cm^3 thf). The progress of the redox conproportionation was monitored by infrared spectroscopy which revealed the conversion of the di- into the tri-anionic cluster. No residual amounts of the tetraanion were detected at any stage of the titration. After completion of the addition of $[N(PPh_3)_2]_4[Os_{20}(CO)_{40}]$ the cluster trianion $[Os_{20}(CO)_{40}]^{3-}$ was the only detectable species in solution. Similar redox titrations were carried out with the other combinations of redox states of **3** represented in equations (1) and (2).

Surface Force-field Study of Cluster **3**.—A quantitative evaluation of the ligand structure of cluster **3** using the coordinates determined in the crystal-structure analysis is precluded by the low accuracy of the positions determined for the light atoms in the compound. This is a general problem in the crystallography of high-nuclearity clusters of heavy metals and a consequence of weak diffraction, lack of high-angle data, strong X-ray scattering by the adjacent heavy atoms and X-ray absorption by the crystalline material. In order to overcome partially these problems, a refined structure of **3** was obtained by a molecular-mechanics simulation on the basis of Lauher's surface force-field method.[16] The most profound effect of the refinement is a consequence of the adjustment of the crystallographically determined C–O and M–C bond distances and M–C–O angles. The bond stretch and M–C–O angle energy is thus almost completely removed in the refinement and the remaining repulsive energy between the carbonyls mainly due to van der Waals and electrostatic interactions of the CO ligands. For the D_{3h} $M_3(CO)_{12}$ and $M(CO)_6$ structures the data of the crystal structures of $[Os_3(CO)_{12}]$ and $[W(CO)_6]$ were similarly refined.[24]

X-Ray Crystallographic Studies of $[AsPh_4]_2[Os_{17}(CO)_{36}]$ **2** *and* $[PBu^n_4]_2[Os_{20}(CO)_{40}]$ **3**.—*Data collection*. Data for cluster **2** were collected on a Philips PW1100 diffractometer with graphite-monochromated Mo-Kα radiation. Unit-cell parameters were determined by a least-squares analysis of 25 automatically centred reflections in the range $8 < \theta < 10°$. Data were collected at 295 K in the range θ 3–21, with a scan width of 0.80° using a technique described previously[25a] and merged to give 6303 reflections with $I/\sigma(I) > 3.0$. Empirical absorption corrections were applied after initial refinement of all atoms with isotropic thermal parameters.

Crystals of the $[PBu^n_4]^+$ salt of cluster **3** were obtained with difficulty and diffracted weakly. Data were collected on a Nicolet R3mV diffractometer with graphite-monochromated Mo-Kα radiation. Unit-cell parameters were determined by a least-squares analysis of 25 automatically centred reflections in the range $10 < \theta < 15°$. Data were collected in the ω–2θ mode at 295 K in the range 2θ 5–38, with a scan width of 1.20°. A total of 8004 reflections were collected and merged to give 6210 independent reflections, 2891 of them with $F > 3\sigma(F)$. Absorption corrections were performed by the ψ-scan method[26] (276 ψ-scan reflections with χ close to 90°), and a linear decay correction was applied.

Table 4 Crystal data and experimental details for $[AsPh_4]_2[Os_{17}(CO)_{36}]$ **2** and $[PBu^n_4]_2[Os_{20}(CO)_{40}]$ **3***

Empirical formula	$C_{84}H_{40}As_2O_{36}Os_{17}$ (0.5 CH_2Cl_2)	$C_{72}H_{72}O_{40}Os_{20}P_2$
M	5050.9	5443.2
Crystal dimensions/mm	0.25 × 0.27 × 0.35	0.05 × 0.11 × 0.21
a/Å	14.836(3)	14.094(5)
b/Å	27.636(6)	16.539(8)
c/Å	12.468(2)	22.650(9)
α/°	97.49(2)	105.93(1)
β/°	96.51(2)	101.788(1)
γ/°	100.11(2)	90.21(1)
U/Å^3	4941	4960
D_{calc}/g cm^{-3}	3.395	3.645
F(000)	4422	4748
μ(Mo-K)α/cm^{-1}	225.6	256.5

* Details in common: triclinic, space group $P\bar{1}$ (no. 2); $Z = 2$.

Structure solution and refinement. The coordinates of the seventeen metal atoms in cluster **2** were obtained by direct methods,[27] and the remaining non-hydrogen atoms were located from subsequent Fourier-difference syntheses. A residual maximum of *ca.* 20 electrons in a Fourier-difference map calculated at this stage was interpreted as an alternative site for Os(17) arising from a small disorder of the cluster. This appeared to correspond to a random distribution of a second orientation of the molecule within the crystal, related to the first by an approximate mirror plane in which all the atoms apart from those associated with Os(17) superimpose in the above structures. The disordered atom Os(17) and its minor component [labelled Os(18) for convenience] were assigned population parameters of 0.84 and 0.16, respectively. The CO groups attached to the minor component were not located. The phenyl rings were given idealised geometry (C–C 1.395, C–H 0.95), with fixed H-atom thermal parameters of 0.08 Å^2. The osmium and arsenic atoms were assigned anisotropic thermal parameters in the final cycles of full-matrix refinement which converged at $R = 0.0773$ and $R' = 0.0799$ with weights of $w = 1/\sigma^2F_o$ assigned to the individual reflections.

The coordinates of the 20 Os atoms of cluster **3** were determined by direct methods. The remaining light atoms (of the carbonyls and $[PBu^n_4]^+$ cations) were located from subsequent Fourier-difference-syntheses. Owing to considerable disorder in the cations, some of the carbon atoms in the $[PBu^n_4]^+$ units could not be detected. All Os atoms were refined anisotropically whereas the atoms in the carbonyl ligands were assigned isotropic thermal parameters. The final cycles of the full-matrix refinement converged at $R = 0.072$, $R' = 0.068$ with weights of $w = [\sigma^2(F) + 0.001F^2]$ assigned to the individual reflections. A final Fourier-difference synthesis was featureless. Fourier-difference syntheses, using either all (6210) or observed data (2891), did not reveal any interstitial atoms in chemically sensible positions.

The data analysis and refinement of clusters **2** and **3** was carried out with the programs of the SHELX 76 and SHELXTL PLUS software packages, respectively.[27,28] Full experimental details are given in Table 4, while the atomic coordinates of the compounds are listed in Tables 5 and 6, respectively.

Additional material available from the Cambridge Crystallographic Data Centre comprises thermal parameters and remaining bond lengths and angles.

Table 5 Fractional atomic coordinates for cluster **2**

Atom	*x*	*y*	*z*	Atom	*x*	*y*	*z*
Os(1)	0.3153(1)	0.2488(1)	0.4883(2)	C(151)	0.3825(57)	0.1192(34)	0.4673(76)
Os(2)	0.3277(1)	0.3046(1)	0.6729(2)	O(151)	0.4480(35)	0.0979(20)	0.4730(46)
Os(3)	0.2861(1)	0.2085(1)	0.6601(2)	C(152)	0.2163(39)	0.0859(24)	0.4931(53)
Os(4)	0.1874(1)	0.3076(1)	0.5222(2)	O(152)	0.1771(36)	0.0449(22)	0.5033(49)
Os(5)	0.1594(1)	0.2635(1)	0.7007(2)	C(153)	0.2582(46)	0.1283(28)	0.3374(65)
Os(6)	0.1465(1)	0.2065(1)	0.4982(2)	O(153)	0.2348(35)	0.1226(21)	0.2236(49)
Os(7)	0.0197(2)	0.2572(1)	0.4139(2)	C(161)	0.4158(58)	0.2606(33)	0.9453(77)
Os(8)	0.0314(1)	0.3151(1)	0.6155(2)	O(161)	0.4828(32)	0.2536(18)	0.9927(43)
Os(9)	−0.0115(1)	0.2140(1)	0.5943(2)	C(162)	0.2449(48)	0.2189(29)	0.9436(65)
Os(10)	0.1850(2)	0.2576(1)	0.3178(2)	O(162)	0.2112(39)	0.1843(24)	0.9992(54)
Os(11)	0.2044(2)	0.3670(1)	0.7216(2)	C(163)	0.3007(45)	0.3186(20)	0.9631(49)
Os(12)	0.1109(1)	0.1599(1)	0.6805(2)	O(163)	0.2942(29)	0.3472(14)	1.0299(34)
Os(13)	0.4672(1)	0.2516(1)	0.6403(2)	C(171)	0.4480(35)	0.3351(21)	0.3698(50)
Os(14)	−0.1411(1)	0.2652(1)	0.5064(2)	O(171)	0.5073(48)	0.3311(28)	0.3191(64)
Os(15)	0.2753(2)	0.1462(1)	0.4671(2)	C(172)	0.3074(53)	0.3891(27)	0.3631(59)
Os(16)	0.3030(2)	0.2624(1)	0.8623(2)	O(172)	0.2934(34)	0.4104(18)	0.2939(40)
Os(17)	0.3440(2)	0.3424(1)	0.4467(3)	C(173)	0.4093(73)	0.3907(41)	0.5470(90)
Os(18)	0.3475(10)	0.3672(6)	0.5282(16)	O(173)	0.4658(45)	0.4146(26)	0.6143(61)
C(11)	0.4071(39)	0.2273(23)	0.4071(54)	As(1)	0.7102(4)	0.0060(2)	0.0759(6)
O(11)	0.4633(34)	0.2205(20)	0.3566(46)	As(2)	0.7524(5)	0.4135(3)	0.0853(7)
C(21)	0.4323(44)	0.3375(26)	0.7786(59)	C(a11)	0.6350(22)	−0.0450(12)	−0.0320(25)
O(21)	0.5017(32)	0.3569(19)	0.8380(44)	C(a12)	0.5913(22)	−0.0337(12)	−0.1281(25)
C(31)	0.3699(60)	0.1785(36)	0.7228(82)	C(a13)	0.5376(22)	−0.0717(12)	−0.2061(25)
O(31)	0.4224(23)	0.1505(14)	0.7721(31)	C(a14)	0.5276(22)	−0.1210(12)	−0.1881(25)
C(41)	0.1513(43)	0.3663(26)	0.4608(60)	C(a15)	0.5712(22)	−0.1323(12)	−0.0920(25)
O(41)	0.1353(32)	0.3978(19)	0.4099(44)	C(a16)	0.6249(22)	−0.0944(12)	−0.0140(25)
C(51)	0.1105(42)	0.2701(24)	0.8410(58)	C(a21)	0.8318(21)	−0.0077(14)	0.0963(33)
O(51)	0.0707(30)	0.2722(17)	0.9128(41)	C(a22)	0.8576(21)	−0.0441(14)	0.0242(33)
C(61)	0.0763(42)	0.1490(26)	0.4178(59)	C(a23)	0.9435(21)	−0.0573(14)	0.0461(33)
O(61)	0.0310(33)	0.1113(19)	0.3455(45)	C(a24)	1.0037(21)	−0.0341(14)	0.1400(33)
C(71)	−0.0578(36)	0.2046(22)	0.3203(50)	C(a25)	0.9779(21)	0.0023(14)	0.2121(33)
O(71)	−0.0162(34)	0.1757(20)	0.2589(46)	C(a26)	0.8919(21)	0.0155(14)	0.1902(33)
C(72)	−0.0188(33)	0.3078(20)	0.3369(46)	C(a31)	0.6614(43)	0.0101(26)	0.2128(60)
O(72)	−0.0423(31)	0.3388(19)	0.2977(42)	C(a32)	0.6052(43)	−0.0298(26)	0.2345(59)
C(81)	−0.0114(42)	0.3684(26)	0.5663(58)	C(a33)	0.5663(42)	−0.0251(25)	0.3329(59)
O(81)	−0.0349(34)	0.4051(21)	0.5461(46)	C(a34)	0.5944(43)	0.0193(26)	0.4208(59)
C(82)	−0.0232(43)	0.3264(25)	0.7438(60)	C(a35)	0.6575(43)	0.0572(26)	0.3909(58)
O(82)	−0.0670(37)	0.3331(21)	0.8100(51)	C(a36)	0.6836(43)	0.0525(26)	0.2788(59)
C(91)	−0.0853(41)	0.2149(26)	0.7083(42)	C(a41)	0.7163(43)	0.0686(25)	0.0252(58)
O(91)	−0.1189(27)	0.2138(17)	0.7847(30)	C(a42)	0.6340(43)	0.0829(26)	−0.0067(59)
C(92)	−0.0868(31)	0.1564(19)	0.5032(43)	C(a43)	0.6315(43)	0.1290(26)	−0.0527(59)
O(92)	−0.1460(39)	0.1242(23)	0.4628(52)	C(a44)	0.7227(42)	0.1569(25)	−0.0694(58)
C(101)	0.1474(72)	0.2985(43)	0.2349(97)	C(a45)	0.8049(43)	0.1353(28)	−0.0326(60)
O(101)	0.1294(41)	0.3329(25)	0.1788(56)	C(a46)	0.8024(44)	0.0954(28)	−0.0057(60)
C(102)	0.2832(36)	0.2531(25)	0.2318(52)	C(b11)	0.8710(27)	0.4527(19)	0.1552(43)
O(102)	0.3354(26)	0.2375(16)	0.1821(35)	C(b12)	0.9080(27)	0.4399(19)	0.2531(43)
C(103)	0.1105(47)	0.1987(28)	0.2225(64)	C(b13)	0.9911(27)	0.4678(19)	0.3104(43)
O(103)	0.0759(45)	0.1679(27)	0.1674(63)	C(b14)	1.0371(27)	0.5085(19)	0.2696(43)
C(111)	0.1597(46)	0.3825(27)	0.8557(64)	C(b15)	1.0002(27)	0.5213(19)	0.1716(43)
O(111)	0.1198(36)	0.3922(21)	0.9283(49)	C(b16)	0.9171(27)	0.4934(19)	0.1144(43)
C(112)	0.1786(48)	0.4255(30)	0.6707(67)	C(b21)	0.7531(40)	0.3445(18)	0.0898(50)
O(112)	0.1639(44)	0.4579(27)	0.6316(61)	C(b22)	0.6851(40)	0.3159(18)	0.1361(50)
C(113)	0.3139(40)	0.4059(23)	0.7869(54)	C(b23)	0.6886(40)	0.2663(18)	0.1438(50)
O(113)	0.3787(37)	0.4314(22)	0.8413(49)	C(b24)	0.7601(40)	0.2454(18)	0.1052(50)
C(121)	0.0367(63)	0.1024(39)	0.6153(83)	C(b25)	0.8280(40)	0.2741(18)	0.0590(50)
O(121)	−0.0146(30)	0.0651(18)	0.5746(40)	C(b26)	0.8245(40)	0.3237(18)	0.0513(50)
C(122)	0.0598(37)	0.1583(22)	0.8120(52)	C(b31)	0.6588(28)	0.4305(19)	0.1546(45)
O(122)	0.0118(33)	0.1567(19)	0.8765(45)	C(b32)	0.5719(28)	0.4270(19)	0.0949(45)
C(123)	0.1984(44)	0.1238(26)	0.7443(59)	C(b33)	0.4993(28)	0.4395(19)	0.1476(45)
O(123)	0.2407(33)	0.0955(20)	0.7730(44)	C(b34)	0.5135(28)	0.4556(19)	0.2601(45)
C(131)	0.5483(28)	0.2997(17)	0.5945(38)	C(b35)	0.6005(28)	0.4591(19)	0.3198(45)
O(131)	0.5987(28)	0.3280(17)	0.5593(38)	C(b36)	0.6731(28)	0.4466(19)	0.2671(45)
C(132)	0.5355(29)	0.2104(18)	0.5900(40)	C(b41)	0.7310(29)	0.4255(20)	−0.0636(33)
O(132)	0.5864(35)	0.1841(21)	0.5537(48)	C(b42)	0.7480(29)	0.3916(20)	−0.1486(33)
C(133)	0.5586(48)	0.2647(28)	0.7746(66)	C(b43)	0.7390(29)	0.4020(20)	−0.2554(33)
O(133)	0.6029(34)	0.2671(19)	0.8564(46)	C(b44)	0.7131(29)	0.4462(20)	−0.2773(33)
C(141)	−0.2116(41)	0.2678(27)	0.6256(44)	C(b45)	0.6961(29)	0.4801(20)	−0.1924(33)
O(141)	−0.2562(27)	0.2743(17)	0.6904(32)	C(b46)	0.7051(29)	0.4697(20)	−0.0855(33)
C(142)	−0.1900(32)	0.3210(20)	0.4351(44)	Cl(1)	0.3030(24)	0.8985(15)	0.3376(34)
O(142)	−0.2252(30)	0.3469(18)	0.4094(41)	Cl(2)	0.2502(20)	0.9915(12)	0.2831(28)
C(143)	−0.2291(51)	0.2197(31)	0.4213(68)	C(Cl)	0.2316(99)	0.9476(76)	0.3131(99)
O(143)	−0.2852(33)	0.1858(20)	0.3706(44)				

Table 6 Atomic coordinates ($\times 10^4$) for cluster **3**

Atom	*x*	*y*	*z*	Atom	*x*	*y*	*z*
Os(1)	3 861(3)	614(3)	3 790(2)	O(121)	1 579	2 635	1 626
Os(2)	4 095(3)	177(3)	1 306(2)	C(122)	3 902	2 335	2 084
Os(3)	2 926(3)	−747(3)	2 841(2)	O(122)	4 568	2 819	2 226
Os(4)	4 902(3)	−664(3)	3 220(2)	C(131)	2 681	1 646	5 109
Os(5)	2 020(3)	277(3)	2 201(2)	O(131)	2 565	1 397	5 547
Os(6)	6 008(3)	−1 903(3)	2 643(2)	C(132)	3 597	2 552	4 741
Os(7)	1 877(3)	545(3)	3 426(2)	O(132)	4 342	3 161	5 128
Os(8)	2 965(3)	1 693(3)	3 119(2)	C(133)	1 861	2 567	4 473
Os(9)	3 138(3)	1 226(3)	624(2)	O(133)	1 385	3 129	4 656
Os(10)	3 953(3)	388(3)	2 551(2)	C(141)	5 465	−1 550	1 224
Os(11)	929(3)	−860(3)	2 528(2)	O(141)	5 647	−2 025	837
Os(12)	3 058(3)	1 457(3)	1 885(2)	C(142)	6 212	−290	2 176
Os(13)	2 828(3)	1 926(3)	4 374(2)	O(142)	7 050	53	2 338
Os(14)	5 054(3)	−838(3)	1 982(2)	C(151)	−1 384	−2 082	1 419
Os(15)	−60(3)	−2 257(3)	1 605(2)	O(151)	−2 119	−1 655	1 280
Os(16)	3 039(3)	−960(3)	1 645(2)	C(152)	−311	−3 169	855
Os(17)	1 979(3)	−2 159(3)	1 946(2)	O(152)	−445	−3 797	443
Os(18)	1 032(3)	−1 110(3)	1 283(2)	C(153)	−642	−2 982	2 051
Os(19)	2 073(3)	51(3)	959(2)	O(153)	−728	−3 282	2 369
Os(20)	3 976(3)	−2 039(3)	2 259(2)	C(161)	3 046	−1 790	815
C(11)	4931	1 402	4 180	O(161)	3 206	−2 182	337
O(11)	5 734	1 676	4 524	C(171)	1 881	−3 049	1 223
C(12)	3 847	87	4 493	O(171)	2 013	−3 655	776
O(12)	3 859	−109	4 861	C(172)	1 738	−2 975	2 468
C(21)	4 348	−590	421	O(172)	1 566	−3 440	2 739
O(21)	4 503	−809	27	C(181)	−50	−635	1 062
C(22)	5 253	1 040	1451	O(181)	−843	−361	925
O(22)	5 880	1 316	1 536	C(182)	974	−1 949	479
C(31)	2 869	−1 322	3 396	O(182)	745	−2 407	−22
O(31)	2 684	−1 749	3 789	C(191)	1 025	676	662
C(41)	6 100	−15	3 646	O(191)	279	934	474
O(41)	6 851	414	3 838	C(192)	1 965	−565	133
C(42)	5 039	−1 166	3 838	O(192)	2 069	−1 026	−332
O(42)	5 102	−1 680	4 202	C(201)	4 184	−2 885	1 618
C(51)	739	959	2 078	O(201)	4 443	−3 434	1 159
O(51)	307	1 344	1 966	C(202)	3 947	−2 709	2 659
C(61)	6 364	−2 754	2 005	O(202)	3 961	−3 033	3 102
O(61)	6 797	−3 246	1 633	P(1)	7 896	−6 745	5 170
C(62)	6 274	−2 683	3 162	C(1A)	7 353	−6 404	5 838
O(62)	6 312	−3 054	3 530	C(2A)	7 062	−6 496	4 458
C(63)	7 462	−1 447	2 993	C(2B)	7 226	−5 388	4 909
O(63)	8 064	−1 097	3 157	C(3A)	8 720	−5 974	5 549
C(71)	705	1 301	3 474	C(3B)	9 398	−6 176	6 033
O(71)	79	1 639	3 512	C(4A)	8 039	−7 939	5 030
C(72)	1 776	22	4 060	C(4B)	8 601	−8 245	4 489
O(72)	1 403	−240	4 426	C(4C)	9 155	−8 999	4 548
C(81)	4 082	2 778	3 549	C(4D)	10 159	−8 733	5 026
O(81)	4 655	3 226	3 817	P(2)	7 635	4 096	1 299
C(82)	1 762	2 337	3 097	C(5A)	7 110	4 204	628
O(82)	1 467	3 024	3 048	C(5B)	7 274	5 069	455
C(91)	3 318	707	−216	C(5C)	6 583	5 250	−107
O(91)	3 137	226	−777	C(5D)	6 798	6 247	−47
C(92)	2 160	1 747	280	C(6A)	8 654	4 454	1 414
O(92)	1 702	2 301	167	C(6B)	9 823	4 429	1 305
C(93)	4 128	1 959	628	C(6C)	9 262	3 960	500
O(93)	4 796	2 386	764	C(7A)	6 918	4 674	1 689
C(101)	5 190	1 101	2910	C(7B)	5 972	4 524	1 677
O(101)	5 804	1 633	3 050	C(7C)	5 125	4 881	2 012
C(111)	489	−1 443	3 046	C(7D)	4 117	4 893	1 853
O(111)	360	−1 797	3 448	C(8A)	7 545	2 901	1 075
C(112)	−275	−356	2 385	C(8B)	6 904	2 771	1 342
O(112)	−1 033	−30	2 473	C(8C)	8 066	2 673	1 960
C(121)	2 229	2 145	1 691				

Acknowledgements

We thank Professor J. W. Lauher for many stimulating discussions as well as Dr. A. J. Amoroso, E. Charalambous and D. C. Coughlin for their help. We acknowledge the financial support of the SERC (to M. McP. and H. R. P.), the British Council, the Kurt Hahn Trust, the Studienstiftung des Deutschen Volkes and ICI plc (to L. H. G.) and the Royal Commission for the Exhibition of 1851 and the U.K. Committee of Vice Chancellors and Principals (to W.-T. W.).

References

1 See, for example, P. Chini, *J. Organomet. Chem.*, 1980, **200**, 37; S. Martinengo, A. Sironi and P. Chini, *J. Am. Chem. Soc.*, 1978, **100**,

7076; G. Ciani, A. Magni, A. Sironi and S. Martinengo, *J. Chem. Soc., Chem. Commun.*, 1981, 1280; S. Martinengo, G. Ciani and A. Sironi, *J. Am. Chem. Soc.*, 1980, **102**, 7564; A. Ceriotti, D. Demartin, G. Longoni, M. Manassero, M. Marchioni, G. Piva and M. Sansoni, *Angew. Chem., Int. Ed. Engl.*, 1985, **24**, 697; A. Ceriotti, A. Fait, G. Longoni, G. Piro, F. Demartin, M. Manassero, N. Masciocchi and M. Sansoni, *J. Am. Chem. Soc.*, 1986, **108**, 8091; A. Fumagalli, S. Martinengo, G. Ciani, N. Masciocchi and A. Sironi, *Inorg. Chem.*, 1992, **31**, 336.

2 L. J. de Jongh, H. B. Brom, G. Longoni, J. M. van Ruitenbeck, G. Schmid, H. H. A. Smit, M. P. Staveren and R. C. Thiel, *New J. Chem.*, 1990, **14**, 559 and refs. therein.

3 G. Ertl, *Gazz. Chim. Ital.*, 1979, **109**, 217; E. L. Muetterties, *Angew. Chem., Int. Ed. Engl.*, 1978, **17**, 545; E. L. Muetterties, T. N. Rodin, E. Band, C. F. Brucker and W. R. Pretzer, *Chem. Rev.*, 1979, **79**, 91; G. A. Somorjai, *J. Phys. Chem.*, 1990, **94**, 1013.

4 J. A. Connor, in *Transition Metal Clusters*, ed. B. F. G. Johnson, Wiley, New York, 1980, p. 345.

5 M. D. Vargas and J. N. Nicholls, *Adv. Inorg. Chem. Radiochem.*, 1986, **30**, 123.

6 T. Chihara, R. Komoto, K. Kobayashi, H. Yamazaki and Y. Matsuura, *Inorg. Chem.*, 1989, **28**, 964; P. J. Bailey, B. F. G. Johnson, J. Lewis, M. McPartlin and H. R. Powell, *J. Organomet. Chem.*, 1989, **377**, C17; P. F. Jackson, B. F. G. Johnson, J. Lewis, M. McPartlin and W. J. H. Nelson, *J. Chem. Soc., Chem. Commun.*, 1980, 224; P. J. Bailey, E. Charalambous, J. Hoyle, B. F. G. Johnson, J. Lewis and M. McPartlin, *J. Chem. Soc., Chem. Commun.*, 1990, 1443; D. M. Washecheck, E. J. Wucherer, L. F. Dahl, A. Ceriotti, G. Longoni, M. Manassero, M. Sansoni and P. Chini, *J. Am. Chem. Soc.*, 1979, **101**, 6110; V. G. Albano, D. Braga, P. Chini, G. Ciani and S. Martinengo, *J. Chem. Soc., Dalton Trans.*, 1982, 645.

7 E. Charalambous, L. H. Gade, B. F. G. Johnson, J. Lewis, M. McPartlin and H. R. Powell, *J. Chem. Soc., Chem. Commun.*, 1990, 688; A. J. Amoroso, L. H. Gade, B. F. G. Johnson, J. Lewis, P. R. Raithby and W.-T. Wong, *Angew. Chem., Int. Ed. Engl.*, 1991, **30**, 107.

8 S. R. Drake, B. F. G. Johnson and J. Lewis, *J. Chem. Soc., Dalton Trans.*, 1988, 1517.

9 P. F. Jackson, B. F. G. Johnson, J. Lewis, W. J. H. Nelson and M. McPartlin, *J. Chem. Soc., Dalton Trans.*, 1982, 2099.

10 R. C. Weast (Editor), *Handbook of Chemistry and Physics*, 70th edn., CRC Press, Boca Raton, FL, 1989/1990, p. F189.

11 A. Bashall, L. H. Gade, J. Lewis, B. F. G. Johnson, G. J. McIntyre and M. McPartlin, *Angew. Chem., Int. Ed. Engl.*, 1991, **30**, 1164.

12 K. Wade, in *Transition Metal Clusters*, ed. B. F. G. Johnson, Wiley, New York, 1980; D. M. P. Mingos, *Acc. Chem. Res.*, 1984, **17**, 311; M. McPartlin, *Polyhedron*, 1984, **3**, 1279.

13 S. Martinengo, A. Fumagalli, R. Bonfichi, G. Ciani and A. Sironi, *J. Chem. Soc., Chem. Commun.*, 1982, 825.

14 P. J. Bailey, M. J. Duer, B. F. G. Johnson, J. Lewis, G. Conole, M. McPartlin, H. R. Powell and C. E. Anson, *J. Organomet. Chem.*, 1990, **383**, 441; L. H. Gade, B. F. G. Johnson and J. Lewis, *J. Chem. Soc., Dalton Trans.*, 1992, 933; P. J. Bailey, L. H. Gade, B. F. G. Johnson and J. Lewis, *Chem. Ber.*, 1992, **125**, 2019.

15 D. M. P. Mingos and Z. Lin, *Chem. Phys.*, 1989, **137**, 15; P. Fantucci and K. Koutecki, in *Elemental and Molecular Clusters*, eds. G. Benedek, T. P. Martin and G. Pacchioni, Springer, Berlin, 1988, p. 125; W. D. Knight, K. Clemenger, W. A. de Heer, W. A. Saunders, M. Y. Chou and M. L. Cohen, *Phys. Rev. Lett.*, 1984, **52**, 2141; M. L. Cohen, M. Y. Chou, W. D. Knight and W. A. de Heer, *J. Phys. Chem.*, 1987, **91**, 3141.

16 J. W. Lauher, *J. Am. Chem. Soc.*, 1986, **108**, 1521.

17 A. J. Amoroso, L. H. Gade, B. F. G. Johnson, J. Lewis and W.-T. Wong, publication in preparation.

18 J. W. Lauher, *J. Am. Chem. Soc.*, 1979, **101**, 2604.

19 B. K. Teo and N. J. A. Sloane, *Inorg. Chem.*, 1985, **24**, 4545.

20 J. W. Lauher, publication in preparation.

21 J. W. Lauher, *J. Am. Chem. Soc.*, 1978, **100**, 5305.

22 B. F. G. Johnson, J. Lewis and D. A. Pippard, *J. Chem. Soc., Dalton Trans.*, 1981, 407.

23 L. H. Gade, B. F. G. Johnson, J. Lewis, M. McPartlin, T. Kotch and A. J. Lees, *J. Am. Chem. Soc.*, 1991, **113**, 8698.

24 M. R. Churchill and B. G. DeBoer, *Inorg. Chem.*, 1977, **16**, 878.

25 (*a*) M. K. Cooper, P. J. Guerney and M. McPartlin, *J. Chem. Soc., Dalton Trans.*, 1982, 757; (*b*) N. Walker and D. Stuart, *Acta Crystallogr., Sect. A*, 1983, **39**, 158.

26 G. Kopfmann and R. Huber, *Acta Crystallogr., Sect. A*, 1968, **24**, 348; A. C. T. North, D. C. Philips and F. S. Matthews, *Acta Crystallogr., Sect. A*, 1968, **24**, 351.

27 G. M. Sheldrick, SHELX 76, Program for Crystal Structure Determination, University of Cambridge, 1976.

28 SHELXTL PLUS™, Release 4.0, Siemens Analytical X-Ray Instruments, Madison, WI, 1990.

Received 7*th September* 1993; *Paper* 3/05355E